

Exciton condensation due to electron-phonon interactionVan-Nham Phan,¹ Klaus W. Becker,² and Holger Fehske³¹*Center of Research and Development, Duy Tan University, K7/25 Quang Trung, Danang, Vietnam*²*Institut für Theoretische Physik, Technische Universität Dresden, D-01062 Dresden, Germany*³*Institut für Physik, Ernst-Moritz-Arndt-Universität Greifswald, D-17489 Greifswald, Germany*

(Received 27 June 2013; revised manuscript received 25 September 2013; published 18 November 2013)

We show that coupling to vibrational degrees of freedom can drive a semimetal excitonic-insulator quantum phase transition in a one-dimensional two-band f - c -electron system at zero temperature. The insulating state typifies an excitonic condensate accompanied by a finite lattice distortion. Using the projector-based renormalization method we analyze the ground-state and spectral properties of the interacting electron-phonon model at half filling. In particular we calculate the momentum dependence of the excitonic order-parameter function and determine the finite critical interaction strength for the metal-insulator transition to appear. The electron spectral function reveals the strong hybridization of f - and c -electron states and the opening of a single-particle excitation gap. The phonon spectral function indicates that the phonon mode involved in the transition softens (hardens) in the adiabatic (nonadiabatic and extreme antiadiabatic) phonon frequency regime.

DOI: [10.1103/PhysRevB.88.205123](https://doi.org/10.1103/PhysRevB.88.205123)

PACS number(s): 71.45.Lr, 71.30.+h, 71.35.Lk, 63.20.kk

I. INTRODUCTION

Low-dimensional electron systems are very susceptible to structural distortions driven by the electron-phonon interaction.¹ Probably the most famous one is the *Peierls instability* of one-dimensional metals,² where the system spontaneously creates a periodic variation in the carrier density at any finite coupling by shifting the ions from their symmetric positions. For the half-filled band case this so-called charge-density wave (CDW) is commensurate with the lattice. Since a static dimerization of the lattice opens a gap at the Fermi surface the metal gives way to an insulator. A full understanding of such a zero-temperature quantum phase transition requires accounting for both quantum lattice fluctuations and strong electronic correlations. For example, it has been found theoretically that quantum fluctuations of the lattice “protect” the metallic state at weak electron-phonon couplings below a finite critical coupling strength.³ An intrasite Coulomb repulsion between electrons of opposite spin, on the other hand, tends to immobilize the carriers but establishes a Mott insulating ground state with strong spin-density correlations instead of the CDW. To analyze the subtle interplay of electron-electron and electron-phonon interaction effects the one-band Holstein-Hubbard model turned out to be particularly rewarding to study.⁴

If we have two electronic bands, however, forming a semimetal with only weak band overlap or a semiconductor with small band gap, the Coulomb interaction between f -band (“hole”) and c -band (“electron”) particles causes the formation of (electron-hole) bound states. Then, at the semimetal-semiconductor transition, the ground state of the crystal may become unstable with respect to the spontaneous formation of excitons. That is, an *excitonic instability* appears,⁵ where the number of free carriers will vary discontinuously under an applied perturbation, signaling a quantum phase transition. The new macroscopic phase-coherent quantum state can be regarded as an electron-hole pair condensate. Worth mentioning, the excitonic state exhibits no “super” transport properties;⁶ rather, it typifies an “excitonic insulator”

(EI) which—under certain conditions—is accompanied by a CDW.⁷ Such a density oscillation can, of course, trigger a lattice distortion which doubles the lattice period, just as for the Peierls state discussed above.

The challenging suggestion of electron-hole pair condensation into the EI phase at equilibrium has been intensively studied within the frameworks of purely electronic, effective-mass Mott-Wannier-type exciton^{8,9} and extended Falicov-Kimball models.^{10–13} In doing, so the coupling to the phonons was neglected. Since the nondistorted semimetal ground state of a simple two-band model with electron and hole Fermi surfaces identical in size and shape is unstable with respect to electron-hole attraction near the semimetal-semiconductor transition, just as the normal Fermi surface of a metal is unstable to the formation of Cooper pairs,⁷ one might ask whether the coupling of electrons and holes to the lattice degrees of freedom alone is sufficient to drive an EI instability. Addressing this question is the primary concern of this paper.

Whether a CDW transition arising from the coupling between valence- and conduction-band electrons is brought about by the electron-electron interaction or by the electron-phonon coupling has been debated for a number of materials in the recent past. For example, in spite of many experimental and theoretical studies, the origin of CDW instability in transition-metal dichalcogenide $1T$ -TiSe₂ remains controversial: it could be the consequence of a novel indirect Jahn-Teller effect,¹⁴ phonon softening,¹⁵ formation of an EI condensate,⁹ or the combination¹⁶ of both the latter scenarios.¹⁷ Also for the mixed-valent rare-earth chalcogenide TmSe_{0.45}Te_{0.55},¹⁸ the lattice degrees of freedom seem to play an important role forming the EI state: very recent heat-capacity measurements indicate that the excitons couple to phonons in the sense of exciton polarons.¹⁹

In this work, we study a one-dimensional two-band f - c -electron model with a coupling to the phonon degrees of freedom only and show that this interaction mediates a “hybridization” between f and c electrons. From a theoretical point of view, we employ both a standard mean-field scheme

and the projector-based renormalization method (PRM).²⁰ The PRM approach, described in Appendix A, includes fluctuation corrections. It enables the calculation of both ground-state and spectral quantities for correlated many-particle systems and furthermore has the ability to find broken-symmetry solutions of phase transitions beyond mean-field theory. We present our numerical results in Sec. V. Our conclusions can be found in Sec. IV.

II. MODEL

Let us consider the following coupled electron-phonon system:

$$\mathcal{H} = \sum_{\mathbf{k}} \varepsilon_{\mathbf{k}}^f f_{\mathbf{k}}^{\dagger} f_{\mathbf{k}} + \sum_{\mathbf{k}} \varepsilon_{\mathbf{k}}^c c_{\mathbf{k}}^{\dagger} c_{\mathbf{k}} + \omega_0 \sum_{\mathbf{q}} b_{\mathbf{q}}^{\dagger} b_{\mathbf{q}} + \frac{g}{\sqrt{N}} \sum_{\mathbf{kq}} [c_{\mathbf{k+q}}^{\dagger} f_{\mathbf{k}} (b_{-\mathbf{q}}^{\dagger} + b_{\mathbf{q}}) + \text{H.c.}], \quad (1)$$

which contains two types of spinless electrons (c, f) carrying momentum \mathbf{k} and dispersionless phonons (b) (see Fig. 1). Here, the electronic excitation energies are given by

$$\varepsilon_{\mathbf{k}}^{f,c} = \varepsilon^{f,c} - t^{f,c} \gamma_{\mathbf{k}} - \mu, \quad (2)$$

whereas ω_0 is the dispersionless phonon energy. In Eq. (2), $\varepsilon^{f,c}$ represents the local part of the respective electronic excitations, and the term $-t^{f,c} \gamma_{\mathbf{k}}$, with $\gamma_{\mathbf{k}} = 2 \cos k$, accounts for a nearest-neighbor hopping in a one-dimensional lattice. Hereafter all energies are given in units of $t^c = 1$. We furthermore note that the electronic energies are measured from the chemical potential μ , where the numerical results presented in Sec. V contain an additional energy shift by fixing $\varepsilon^c = 0$. The last term in Eq. (1) describes a local electron-phonon interaction (with coupling constant g), written in \mathbf{k} space, between local

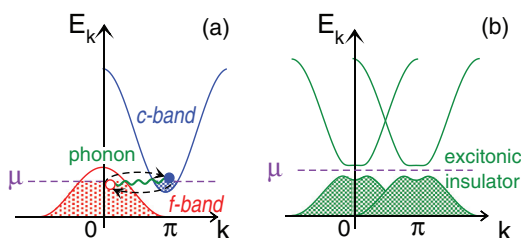


FIG. 1. (Color online) (a) Semimetallic f - c -electron band structure used in this work. An f valence-band hole and a c conduction-band electron may form an “excitonic” bound state owing to their interaction with the lattice degrees of freedom, with a Brillouin-zone boundary phonon involved for momentum-conservation reasons. Note that the schematic band structure shown mimics the situation in the EI material $\text{TmSe}_{0.45}\text{Te}_{0.55}$, where the quasilocalized $4f^{13}$ state has its maximum at the Γ point, the $5d$ strongly dispersive state has its minimum at the X point, and exciton formation is accompanied by a Γ - X phonon.¹⁹ Also in $1T$ - TiSe_2 the valence-band top and the conduction-band minimum are located at different points in the Brillouin zone.²¹ (b) For the case in which, above a critical electron-phonon coupling strength f - c -electron coherence is achieved at sufficiently low temperatures, even a new symmetry-broken ground state may appear, the so-called excitonic insulator, which may be accompanied by a finite lattice distortion and a modulation of the charge density.⁷

f - c particle-hole excitations and lattice displacements. Apparently it represents an effective “exciton”-phonon interaction. In Eq. (1) we have introduced Fourier-transformed quantities $f_{\mathbf{k}}^{\dagger} = (1/\sqrt{N}) \sum_i f_i^{\dagger} e^{i\mathbf{k}\mathbf{R}_i}$, $c_{\mathbf{k}}^{\dagger} = (1/\sqrt{N}) \sum_i c_i^{\dagger} e^{i\mathbf{k}\mathbf{R}_i}$, and $b_{\mathbf{q}}^{\dagger} = (1/\sqrt{N}) \sum_i b_i^{\dagger} e^{i\mathbf{q}\mathbf{R}_i}$, where $f_i^{\dagger}, c_i^{\dagger}$, and b_i^{\dagger} are the local quantities. N counts the number of lattice sites i .

In what follows, we consider a half-filled band, i.e.,

$$n = \langle n_i^f \rangle + \langle n_i^c \rangle = 1, \quad (3)$$

where $n_i^f = (1/N) \sum_{\mathbf{k}} f_{\mathbf{k}}^{\dagger} f_{\mathbf{k}}$ and $n_i^c = (1/N) \sum_{\mathbf{k}} c_{\mathbf{k}}^{\dagger} c_{\mathbf{k}}$. The chemical potential μ has to be adjusted in such a way that Eq. (3) is satisfied. Without loss of generality, in what follows, the c electrons will be considered as “light” while the f electrons (respectively holes) are “heavy,” i.e., $|t^f| < 1$. For negative t^f , and coinciding energies of c and f electrons, one is led to a picture of indirect c - f hopping (cf. Fig. 1), which suggests a possible condensation of bound c - f -electron-hole pairs with finite momentum:

$$d_{\mathbf{k}} = \langle c_{\mathbf{k+Q}}^{\dagger} f_{\mathbf{k}} \rangle \neq 0, \quad (4)$$

where $\mathbf{Q} = \pi$ in one dimension. Allowing broken-symmetry solutions for nonvanishing $d_{\mathbf{k}}$, small infinitesimal fields must be included in model Eq. (1). We write

$$\mathcal{H} = \sum_{\mathbf{k}} \varepsilon_{\mathbf{k}}^f f_{\mathbf{k}}^{\dagger} f_{\mathbf{k}} + \sum_{\mathbf{k}} \varepsilon_{\mathbf{k}}^c c_{\mathbf{k}}^{\dagger} c_{\mathbf{k}} + \omega_0 \sum_{\mathbf{q}} b_{\mathbf{q}}^{\dagger} b_{\mathbf{q}} + \Delta_0 \sum_{\mathbf{k}} (c_{\mathbf{k+Q}}^{\dagger} f_{\mathbf{k}} + f_{\mathbf{k}}^{\dagger} c_{\mathbf{k+Q}}) + \sqrt{N} h_0 (b_{-\mathbf{Q}}^{\dagger} + b_{\mathbf{Q}}) + \frac{g}{\sqrt{N}} \sum_{\mathbf{kq}} [c_{\mathbf{k+q}}^{\dagger} f_{\mathbf{k}} (b_{-\mathbf{q}}^{\dagger} + b_{\mathbf{q}}) + \text{H.c.}], \quad (5)$$

where $\Delta_0 = 0^+$ and $h_0 = 0^+$. It is easily realized that the fields h_0 and Δ_0 are mutually dependent. Moreover, since $b_{\mathbf{Q}} = b_{-\mathbf{Q}}$ the field contribution $\sqrt{N} h_0 (b_{-\mathbf{Q}}^{\dagger} + b_{\mathbf{Q}})$ can be replaced by $\sqrt{N} h_0 (b_{-\mathbf{Q}}^{\dagger} + b_{-\mathbf{Q}})$. Therefore a finite lattice displacement $\propto \langle b_{-\mathbf{Q}}^{\dagger} + b_{-\mathbf{Q}} \rangle$ would give rise to the formation of a charge-density wave connected to a doubling of the lattice unit cell.

III. MEAN-FIELD THEORY

To solve model Eq. (5) in mean-field approximation it is advantageous first to introduce fluctuation operators $\delta\mathcal{A} = \mathcal{A} - \langle \mathcal{A} \rangle$ in the electron(exciton)-phonon interaction. Using

$$\begin{aligned} & \delta(c_{\mathbf{k+q}}^{\dagger} f_{\mathbf{k}}) \delta(b_{-\mathbf{q}}^{\dagger} + b_{\mathbf{q}}) \\ &= c_{\mathbf{k+q}}^{\dagger} f_{\mathbf{k}} (b_{-\mathbf{q}}^{\dagger} + b_{\mathbf{q}}) - [\langle c_{\mathbf{k+q}}^{\dagger} f_{\mathbf{k}} \rangle (b_{-\mathbf{q}}^{\dagger} + b_{\mathbf{q}}) \\ &+ c_{\mathbf{k+q}}^{\dagger} f_{\mathbf{k}} \langle b_{-\mathbf{q}}^{\dagger} + b_{\mathbf{q}} \rangle] \delta_{\mathbf{q},\mathbf{Q}} + \langle c_{\mathbf{k+q}}^{\dagger} f_{\mathbf{k}} \rangle \langle b_{-\mathbf{q}}^{\dagger} + b_{\mathbf{q}} \rangle \delta_{\mathbf{q},\mathbf{Q}}, \end{aligned} \quad (6)$$

the Hamiltonian \mathcal{H} is best rewritten as

$$\mathcal{H} = \mathcal{H}_0 + \mathcal{H}_1 \quad (7)$$

with

$$\begin{aligned} \mathcal{H}_0 = & \sum_{\mathbf{k}} \varepsilon_{\mathbf{k}}^f f_{\mathbf{k}}^\dagger f_{\mathbf{k}} + \sum_{\mathbf{k}} \varepsilon_{\mathbf{k}}^c c_{\mathbf{k}}^\dagger c_{\mathbf{k}} + \omega_0 \sum_{\mathbf{q}} b_{\mathbf{q}}^\dagger b_{\mathbf{q}} \\ & + \Delta \sum_{\mathbf{k}} (c_{\mathbf{k}+\mathbf{Q}}^\dagger f_{\mathbf{k}} + f_{\mathbf{k}}^\dagger c_{\mathbf{k}+\mathbf{Q}}) + \sqrt{N} h (b_{-\mathbf{Q}}^\dagger + b_{-\mathbf{Q}}), \end{aligned} \quad (8)$$

$$\mathcal{H}_1 = \frac{g}{\sqrt{N}} \sum_{\mathbf{k}, \mathbf{q}} [\delta(c_{\mathbf{k}+\mathbf{q}}^\dagger f_{\mathbf{k}}) \delta(b_{-\mathbf{q}}^\dagger + b_{\mathbf{q}}) + \text{H.c.}]. \quad (9)$$

Here the fields have acquired additional shifts, which will act as order parameters in the following:

$$\Delta = \Delta_0 + \frac{g}{\sqrt{N}} \langle b_{-\mathbf{Q}} + b_{-\mathbf{Q}}^\dagger \rangle, \quad (10)$$

$$h = h_0 + \frac{g}{N} \sum_{\mathbf{k}} \langle c_{\mathbf{k}+\mathbf{Q}}^\dagger f_{\mathbf{k}} + f_{\mathbf{k}}^\dagger c_{\mathbf{k}+\mathbf{Q}} \rangle, \quad (11)$$

where the infinitesimal $\Delta_0 = 0^+$ and $h_0 = 0^+$ can be neglected for finite expectation values on the right-hand sides.

Finally, we eliminate in Eq. (8) the term $\propto (b_{-\mathbf{Q}}^\dagger + b_{-\mathbf{Q}})$ by defining new phonon operators:

$$B_{\mathbf{q}}^\dagger = b_{\mathbf{q}}^\dagger + \sqrt{N} (h/\omega_0) \delta_{\mathbf{q}, \mathbf{Q}}, \quad (12)$$

where the definition is independent of the sign of \mathbf{Q} . \mathcal{H}_0 and \mathcal{H}_1 then become

$$\begin{aligned} \mathcal{H}_0 = & \sum_{\mathbf{k}} \varepsilon_{\mathbf{k}}^f f_{\mathbf{k}}^\dagger f_{\mathbf{k}} + \sum_{\mathbf{k}} \varepsilon_{\mathbf{k}}^c c_{\mathbf{k}}^\dagger c_{\mathbf{k}} + \omega_0 \sum_{\mathbf{q}} B_{\mathbf{q}}^\dagger B_{\mathbf{q}} \\ & + \Delta \sum_{\mathbf{k}} (c_{\mathbf{k}+\mathbf{Q}}^\dagger f_{\mathbf{k}} + f_{\mathbf{k}}^\dagger c_{\mathbf{k}+\mathbf{Q}}) + \text{const}, \end{aligned} \quad (13)$$

$$\mathcal{H}_1 = \frac{g}{\sqrt{N}} \sum_{\mathbf{k}, \mathbf{q}} [\delta(c_{\mathbf{k}+\mathbf{q}}^\dagger f_{\mathbf{k}}) \delta(B_{-\mathbf{q}}^\dagger + B_{\mathbf{q}}) + \text{H.c.}]. \quad (14)$$

In \mathcal{H}_1 we have used $\delta B_{-\mathbf{q}}^\dagger = \delta b_{-\mathbf{q}}^\dagger$ and $\delta B_{\mathbf{q}} = \delta b_{\mathbf{q}}$.

Note that the Hamiltonian $\mathcal{H} = \mathcal{H}_0 + \mathcal{H}_1$, with \mathcal{H}_0 and \mathcal{H}_1 given by Eqs. (13) and (14), is still exact. The Hamiltonian in mean-field approximation is obtained by completely neglecting the fluctuation part \mathcal{H}_1 . Thus the mean-field Hamiltonian reads

$$\begin{aligned} \mathcal{H}_{\text{MF}} = & \sum_{\mathbf{k}} \varepsilon_{\mathbf{k}}^f f_{\mathbf{k}}^\dagger f_{\mathbf{k}} + \sum_{\mathbf{k}} \varepsilon_{\mathbf{k}}^c c_{\mathbf{k}}^\dagger c_{\mathbf{k}} + \omega_0 \sum_{\mathbf{q}} B_{\mathbf{q}}^\dagger B_{\mathbf{q}} \\ & + \Delta \sum_{\mathbf{k}} (c_{\mathbf{k}+\mathbf{Q}}^\dagger f_{\mathbf{k}} + f_{\mathbf{k}}^\dagger c_{\mathbf{k}+\mathbf{Q}}), \end{aligned} \quad (15)$$

where the constant from Eq. (13) will be suppressed. The electronic part of \mathcal{H}_{MF} is diagonalized by use of a Bogoliubov transformation. Then \mathcal{H}_{MF} is rewritten as

$$\mathcal{H}_{\text{MF}} = \sum_{\mathbf{k}} E_{\mathbf{k}}^{(1)} C_{1,\mathbf{k}}^\dagger C_{1,\mathbf{k}} + \sum_{\mathbf{k}} E_{\mathbf{k}}^{(2)} C_{2,\mathbf{k}}^\dagger C_{2,\mathbf{k}} + \omega_0 \sum_{\mathbf{q}} B_{\mathbf{q}}^\dagger B_{\mathbf{q}}, \quad (16)$$

where the electronic quasiparticle energies and quasiparticles operators read

$$E_{\mathbf{k}}^{(1,2)} = \frac{\varepsilon_{\mathbf{k}+\mathbf{Q}}^c + \varepsilon_{\mathbf{k}}^f}{2} \mp \frac{\text{sgn}(\varepsilon_{\mathbf{k}}^f - \varepsilon_{\mathbf{k}+\mathbf{Q}}^c)}{2} W_{\mathbf{k}}, \quad (17)$$

and

$$C_{1,\mathbf{k}}^\dagger = \xi_{\mathbf{k}} c_{\mathbf{k}+\mathbf{Q}}^\dagger + \eta_{\mathbf{k}} f_{\mathbf{k}}^\dagger, \quad (18)$$

$$C_{2,\mathbf{k}}^\dagger = -\eta_{\mathbf{k}} c_{\mathbf{k}+\mathbf{Q}}^\dagger + \xi_{\mathbf{k}} f_{\mathbf{k}}^\dagger. \quad (19)$$

Here the prefactors are given by

$$\xi_{\mathbf{k}}^2 = \frac{1}{2} \left[1 + \text{sgn}(\varepsilon_{\mathbf{k}}^f - \varepsilon_{\mathbf{k}+\mathbf{Q}}^c) \frac{\varepsilon_{\mathbf{k}}^f - \varepsilon_{\mathbf{k}+\mathbf{Q}}^c}{W_{\mathbf{k}}} \right], \quad (20)$$

$$\eta_{\mathbf{k}}^2 = \frac{1}{2} \left[1 - \text{sgn}(\varepsilon_{\mathbf{k}}^f - \varepsilon_{\mathbf{k}+\mathbf{Q}}^c) \frac{\varepsilon_{\mathbf{k}}^f - \varepsilon_{\mathbf{k}+\mathbf{Q}}^c}{W_{\mathbf{k}}} \right], \quad (21)$$

with

$$W_{\mathbf{k}} = \sqrt{(\varepsilon_{\mathbf{k}+\mathbf{Q}}^c - \varepsilon_{\mathbf{k}}^f)^2 + 4|\Delta|^2}. \quad (22)$$

The quadratic form of Eq. (16) allows us to compute all expectation values formed with \mathcal{H}_{MF} . From Eqs. (10)–(12) one easily obtains the following implicit equation for the order parameters $\Delta = -(2g/\omega_0)h$:

$$1 = \frac{4g^2}{\omega_0} \frac{1}{N} \sum_{\mathbf{k}} \text{sgn}(\varepsilon_{\mathbf{k}}^f - \varepsilon_{\mathbf{k}+\mathbf{Q}}^c) \frac{f^F(E_{\mathbf{k}}^{(1)}) - f^F(E_{\mathbf{k}}^{(2)})}{W_{\mathbf{k}}}. \quad (23)$$

Here $f^F(E_{\mathbf{k}}^{(1,2)})$ are Fermi functions, which—working at zero temperature in what follows—reduce to the corresponding Θ functions. Note that Eq. (23) represents a BCS-like equation for Δ . A nonzero Δ accounts for an exciton condensation phase as was explained above. In Figs. 3 and 4 below, it will be shown that such a phase occurs for a sufficiently large coupling constant $g > g_c^{\text{MF}}(\omega_0)$. We would already like to point out here that the critical coupling constant g_c^{MF} is generally smaller than the corresponding g_c^{PRM} , obtained below by including fluctuation processes.

Let us also consider the one-particle spectral function $A_{\mathbf{k}}^{(c,f)}(\omega)$ for c and f electrons. For c electrons it is defined by

$$A_{\mathbf{k}}^c(\omega) = \frac{1}{2\pi} \int_{-\infty}^{\infty} \langle [c_{\mathbf{k}\sigma}(t), c_{\mathbf{k}\sigma}^\dagger]_+ \rangle e^{i\omega t} dt, \quad (24)$$

where the expectation value is formed with \mathcal{H}_{MF} . For $A^c(\mathbf{k}, \omega)$ and the corresponding equation for the f electrons one finds

$$A_{\mathbf{k}}^c(\omega) = \xi_{\mathbf{k}-\mathbf{Q}}^2 \delta(\omega - E_{\mathbf{k}-\mathbf{Q}}^{(1)}) + \eta_{\mathbf{k}-\mathbf{Q}}^2 \delta(\omega - E_{\mathbf{k}-\mathbf{Q}}^{(2)}), \quad (25)$$

$$A_{\mathbf{k}}^f(\omega) = \eta_{\mathbf{k}}^2 \delta(\omega - E_{\mathbf{k}}^{(1)}) + \xi_{\mathbf{k}}^2 \delta(\omega - E_{\mathbf{k}}^{(2)}). \quad (26)$$

Thus both spectral functions are built up by two coherent excitations with energies $E_{\mathbf{k}}^{(1)}$ and $E_{\mathbf{k}}^{(2)}$. Finally, the phonon spectral function

$$C_{\mathbf{q}}(\omega) = \frac{1}{2\pi\omega} \int_{-\infty}^{\infty} \langle [b_{\mathbf{q}}(t), b_{\mathbf{q}}^\dagger] \rangle e^{i\omega t} dt \quad (27)$$

is given by

$$C_{\mathbf{q}}(\omega) = \frac{\delta(\omega - \omega_0)}{\omega_0}, \quad (28)$$

which shows a \mathbf{q} -independent excitation at $\omega = \omega_0$. Note that, in contrast to the electronic excitations in Eqs. (25) and (26), the phonon frequency ω_0 is not changed in mean-field approximation.

IV. FLUCTUATION CORRECTIONS BEYOND MEAN-FIELD THEORY

In the mean-field treatment above, fluctuation processes from the interaction \mathcal{H}_1 have completely been left out. In the

following, we therefore apply the PRM²⁰ to evaluate the order parameters, the one-particle spectral functions $A_{\mathbf{k}}^{(c,f)}(\omega)$, and the phonon spectral function $C_{\mathbf{q}}(\omega)$ for the case that \mathcal{H}_1 is included. To avoid technical details, the explicit application is shifted to Appendix A. The general concept of the PRM is as follows: The presence of the interaction \mathcal{H}_1 prevents a straightforward solution of the Hamiltonian $\mathcal{H} = \mathcal{H}_0 + \mathcal{H}_1$. For that reason the Hamiltonian is transformed into a diagonal (or at least quasideagonal) form by applying a sequence of small unitary transformations to \mathcal{H} . Denoting for a moment the generator of the whole sequence by $X = -X^\dagger$, in Appendix A it is shown that one can arrive at an effective Hamiltonian $\tilde{\mathcal{H}} = e^X \mathcal{H} e^{-X}$, which has the same operator structure as Hamiltonian \mathcal{H}_0 in Eq. (13):

$$\begin{aligned} \tilde{\mathcal{H}} = & \sum_{\mathbf{k}} \tilde{\varepsilon}_{\mathbf{k}}^f f_{\mathbf{k}}^\dagger f_{\mathbf{k}} + \sum_{\mathbf{k}} \tilde{\varepsilon}_{\mathbf{k}}^c c_{\mathbf{k}}^\dagger c_{\mathbf{k}} + \sum_{\mathbf{q}} \tilde{\omega}_{\mathbf{q}} B_{\mathbf{q}}^\dagger B_{\mathbf{q}} \\ & + \tilde{\Delta} \sum_{\mathbf{k}} (c_{\mathbf{k}+\mathbf{Q}}^\dagger f_{\mathbf{k}} + f_{\mathbf{k}}^\dagger c_{\mathbf{k}+\mathbf{Q}}). \end{aligned} \quad (29)$$

Here, $\tilde{\varepsilon}_{\mathbf{k}}^f$, $\tilde{\varepsilon}_{\mathbf{k}}^c$, $\tilde{\omega}_{\mathbf{q}}$, and $\tilde{\Delta}$ are renormalized parameters, which have to be determined self-consistently by taking into account contributions to infinite order in the interaction \mathcal{H}_1 . Also, the phonon frequency $\tilde{\omega}_{\mathbf{q}}$ has acquired a \mathbf{q} dependence. Note that the PRM ensures a well-controlled disentanglement of higher-order interaction terms which enter in the elimination procedure.

The PRM also allows us to evaluate expectation values $\langle \mathcal{A} \rangle$, formed with the full Hamiltonian \mathcal{H} . Thereby, one uses the property of unitary invariance of operator expressions under a trace. Employing the same unitary transformation to \mathcal{A} as before for the Hamiltonian, one finds $\langle \mathcal{A} \rangle = \langle \tilde{\mathcal{A}} \rangle_{\tilde{\mathcal{H}}}$, where the expectation value is formed with $\tilde{\mathcal{H}}$ and $\tilde{\mathcal{A}} = e^X \mathcal{A} e^{-X}$. Note that Hamiltonian $\tilde{\mathcal{H}}$ from Eq. (29) can be transformed into a diagonal form by use of a Bogoliubov transformation in analogy to the transformation from Eq. (15) to Eq. (16). Therefore, any expectation value, formed with $\tilde{\mathcal{H}}$, can be evaluated exactly.

As an example, let us consider the spectral function $A_{\mathbf{k}}^c(\omega)$ from the former expression Eq. (24), where the expectation value should however be formed with the full Hamiltonian \mathcal{H} (and not with \mathcal{H}_{MF}). Applying the unitary invariance of operator expressions under a trace, $A_{\mathbf{k}}^c(\omega)$ is rewritten as

$$A_{\mathbf{k}}^c(\omega) = \frac{1}{2\pi} \int_{-\infty}^{\infty} \langle [\tilde{c}_{\mathbf{k}\sigma}(t), \tilde{c}_{\mathbf{k}\sigma}^\dagger]_+ \rangle_{\tilde{\mathcal{H}}} e^{i\omega t} dt, \quad (30)$$

where the expectation value is now formed with $\tilde{\mathcal{H}}$ instead of with \mathcal{H} . Correspondingly $\tilde{c}_{\mathbf{k}\sigma}^\dagger$ and $\tilde{c}_{\mathbf{k}\sigma}$ are the transformed electron operators, $\tilde{c}_{\mathbf{k}\sigma}^{(\dagger)} = e^X c_{\mathbf{k}\sigma}^{(\dagger)} e^{-X}$, and the time dependence is governed by $\tilde{\mathcal{H}}$ as well.

V. NUMERICAL RESULTS

A. Ground-state properties

We start with a discussion of the EI order parameter Δ and the corresponding lattice displacement x_Q in the ground state of the fully renormalized two-band model Eq. (A25) in one dimension. Figure 2 at first displays the profile of the excitonic expectation value d_k , in dependence on the electron-phonon

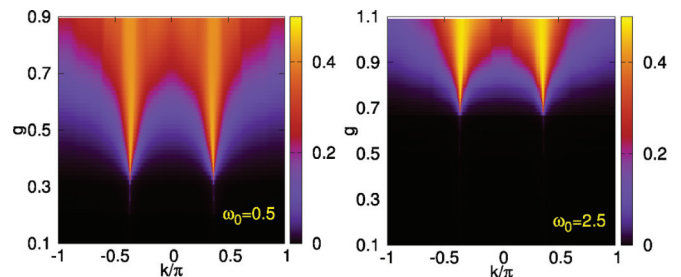


FIG. 2. (Color online) Magnitude of the EI order-parameter function $d_k = \langle c_{k+Q}^\dagger f_k \rangle$ with $Q = \pi$ (cf. color bar) depending on momentum k (on the x axis) and the electron-phonon coupling strength g (on the y axis) in the adiabatic ($\omega_0 = 0.5$, left-hand panel) and nonadiabatic ($\omega_0 = 2.5$, right-hand panel) phonon frequency regime.

coupling g , for two characteristic phonon frequencies ω_0 describing adiabatic ($\omega_0 < 1$) and nonadiabatic ($\omega_0 > 1$) situations. This quantity designates the range in momentum space where c electrons and f holes are perceptibly involved in the electron-hole pair formation and exciton condensation process. Obviously d_k vanishes (within numerical accuracy) for all k below a critical coupling strength [$g_c \simeq 0.28$ (0.6) at $\omega_0 = 0.5$ (2.5)]. At and just above the critical coupling d_k is solely finite at and near the Fermi momentum k_F , respectively, indicating a BCS-type electron-hole pairing instability. A further increasing electron-phonon coupling implicates more and more electron and hole states in the pairing process up to the point where Fermi-surface (nesting) effects are ineffectual. Thus we expect that local, tightly bound excitons will form in the strong interaction limit and, as a consequence, Bose-Einstein rather than BCS-like condensation takes place.^{8,13} This regime is beyond our weak-coupling PRM approach, however.

Figure 3 now gives Δ and x_Q as a function of g for $\omega_0 = 0.5$ and 2.5 and shows the precision with which the critical coupling can be determined. We see that Δ and x_Q are intimately related; while the semimetal corresponds to an

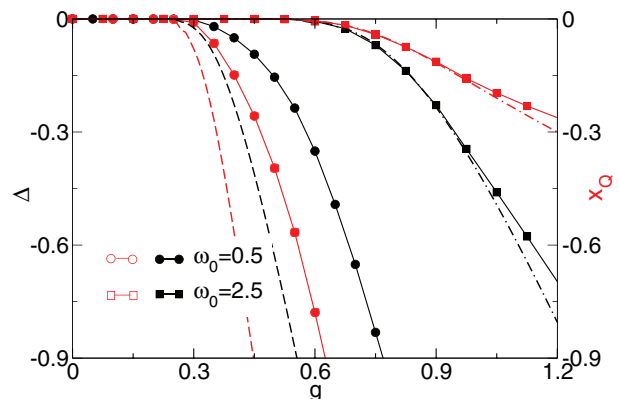


FIG. 3. (Color online) EI order parameter Δ (black filled symbols, left axis of ordinate) and lattice displacement x_Q (red open symbols, right axis of ordinate) as functions of the electron-phonon interaction g in the adiabatic ($\omega_0 = 0.5$, circles) and nonadiabatic ($\omega_0 = 2.5$, squares) cases. Black (red) dashed (dot-dashed) lines without symbols give the corresponding mean-field results for Δ (x_Q) at $\omega_0 = 0.5$ ($\omega_0 = 2.5$).

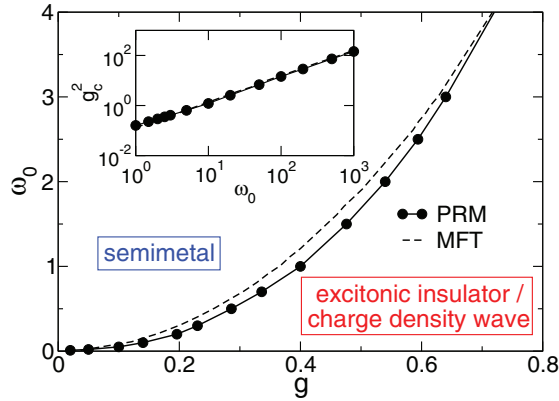


FIG. 4. (Color online) PRM ground-state phase diagram of the two-band f - c -electron-phonon model in the g - ω_0 plane for the half-filled band case. Inset: Asymptotic behavior of the (squared) critical coupling strength g_c^2 at very large phonon frequencies ($\omega_0 \rightarrow \infty$) (cf. Appendix B). Dashed lines give the corresponding mean-field results.

undistorted ground state, the EI or CDW state exhibits a finite lattice distortion (dimerization). Actually, we expect that the semimetal-EI transition is of Kosterlitz-Thouless type,²² at least in the antiadiabatic ($\omega_0 \gg 1$) regime. If so, the charge gap will open exponentially on entering the insulating phase, in line with what is observed for the (repulsive Tomonaga-Luttinger liquid) metal-CDW transition in the one-dimensional spinless fermion Holstein^{23,24} and Edwards²⁵ models. Also, in conformity with the Holstein model we find that quantum phonon fluctuations protract the metal-insulator transition, which takes place at infinitesimal small coupling only if $\omega_0 \rightarrow 0$. The effect of fluctuations beyond mean field is obvious: within the PRM scheme a larger electron-phonon coupling g is required to achieve the same magnitude of the EI order or lattice displacement. The difference between PRM and mean-field results is insignificant, of course, for very large phonon frequencies.

The derived zero-temperature quantum phase transition lines, separating the semimetallic and EI phases in the g - ω_0 plane, are shown in Fig. 4. In the intermediate coupling and frequency regime, we observe distinct PRM corrections to the mean-field transition points. In the antiadiabatic limit ($\omega_0 \rightarrow \infty$), where the phononic degrees of freedom can be integrated out, the squared critical coupling g_c^2 scales linearly with ω_0 , and we find $(g_c^2/\omega_0)_{\omega_0 \rightarrow \infty} \simeq 0.14$ (see inset). Here the phase boundary basically agrees with that of mean-field theory (cf. Fig. 4). An analytical proof of this finding is given in Appendix B.

B. Spectral properties

We now present the PRM results for the single-particle spectral functions associated with the photoemission or inverse photoemission (injection) of a c or f electron with wave number k and energy ω , which serve as a direct measures of the occupied and unoccupied states. Figure 5 shows the variation of $A_k^{c,f}(\omega)$ as the electron-phonon coupling increases in the adiabatic regime. For weak couplings (see upper panels), we are in the semimetallic phase, and $A_k^{c,f}(\omega)$ reflect the weakly renormalized c - and f -band dispersions (note that

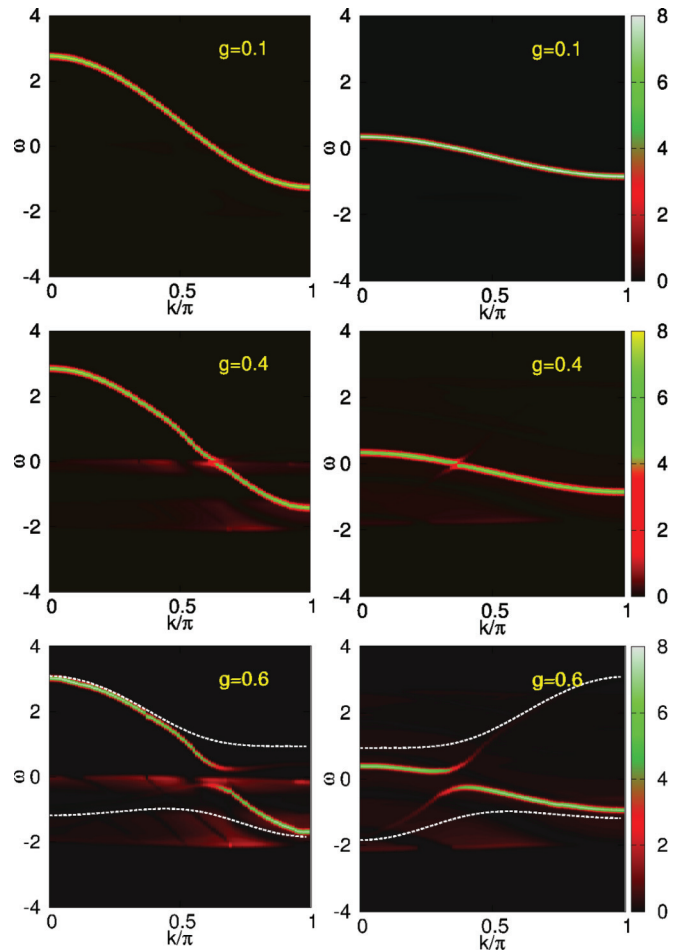


FIG. 5. (Color online) Intensity plots of the c -electron (left-hand panels) and f -electron (right-hand panels) single-particle spectral functions $A_k^{c,f}(\omega)$ in the adiabatic regime with $\omega_0 = 0.5$. The electron-phonon coupling g increases as indicated from top to bottom panels. In the lowermost two panels the corresponding mean-field results are included, without dissolving the spectral intensity however (see white dashed lines).

the energy ω is measured with respect to the Fermi energy). In the EI phase, a gap opens at the Fermi energy and we observe a pronounced backfolding of the spectral signature at larger coupling. Here c - and f -electron states strongly hybridize close to the Fermi energy. The same, in principle, holds in the nonadiabatic regime. However, for the parameters used in Fig. 6, the ratio $g/\omega_0 = 0.32$ is much smaller than for the EI phase depicted in the two lowermost panels of Fig. 5 where $g/\omega_0 = 1.2$. Hence multiphonon processes are less important in the former case and—prescinding from the gap feature—the photoemission spectrum is less affected by the lattice degrees of freedom. For comparison, we show also the outcome of mean-field theory for $A_k^c(\omega)$ and $A_k^f(\omega)$ in lower panels where $g = 0.6$. We see that the band gap is considerably overestimated, and there is, of course, no incoherent contribution at all.

More information in this respect comes from the phonon spectral function $C_q(\omega)$, represented in Fig. 7, below (upper panels) and above (lower panels) the semimetal-EI transition point. At weak coupling, the absorption signal is dominated

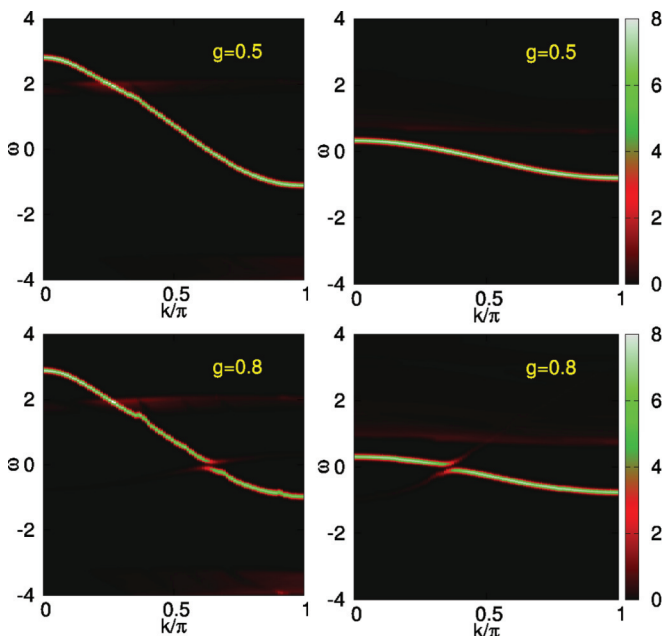


FIG. 6. (Color online) Intensity plots of the c -electron (left-hand panels) and f -electron (right-hand panels) single-particle spectral functions $A_k^{c,f}(\omega)$ for $g = 0.5$ (top panels) and $g = 0.8$ (bottom panels) in the nonadiabatic regime with $\omega_0 = 2.5$.

by the coherent part of $C_q(\omega)$, which is almost dispersionless and located near the bare phonon frequency, i.e., $\tilde{\omega}_q \simeq \omega_0$. This particularly holds for the case $g = 0.1$, $\omega_0 = 0.5$ shown in the top left panel. For $g = 0.5$ and a higher phonon frequency $\omega_0 = 2.5$, the overall intensity of the signal goes down, of course. Note that the phonon mode acquires a slight dispersion: It becomes larger near the Brillouin-zone boundary

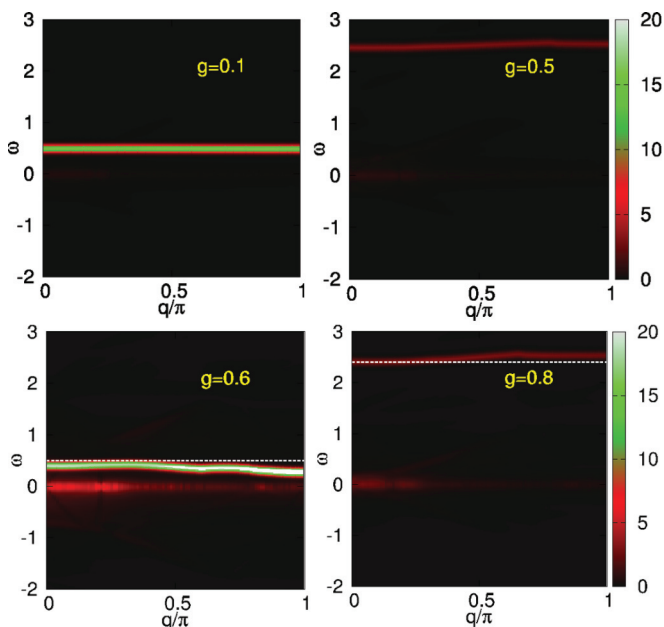


FIG. 7. (Color online) Intensity plots of the phonon spectral function $C_q(\omega)$ for different g at $\omega_0 = 0.5$ (left-hand panels) and $\omega_0 = 2.5$ (right-hand panels). The straight white dashed line in the lower panels marks the dispersionless mean-field result.

($\tilde{\omega}_\pi \gtrsim \omega_0$). Above the transition [$g > g_c(\omega_0)$], we observe two distinct features [see lower panels of Fig. 7]. First, the phonon mode softens for $\omega_0 = 0.5$ while it hardens for $\omega_0 = 2.5$. That is, we find an opposite tendency for small and large phonon frequencies. This result can already be understood from perturbation theory for the phonon energy as shown in Appendix A 4. Second, a new signal at $\omega = 0$ appears which indicates the strong coupling between electronic and phononic degrees of freedom. Note that the phonon spectral function calculated within mean-field approximation shows only a single dispersionless signal at $\omega = \omega_0$.

Besides coherent excitations all spectral functions in Figs. 5–7 also show incoherent excitations. They can be detected as (red) much weaker developed contributions which deviate from the coherent ones. They possess two general features: (i) Their weight increases with increasing electron-phonon coupling g since they are induced by \mathcal{H}_1 , and (ii) their weight is strongly suppressed in the adiabatic limit. This is explained in Appendix B. To elucidate the distribution of the spectral weight in more detail, we show in Fig. 8 the coherent (left) and incoherent (right) part of the

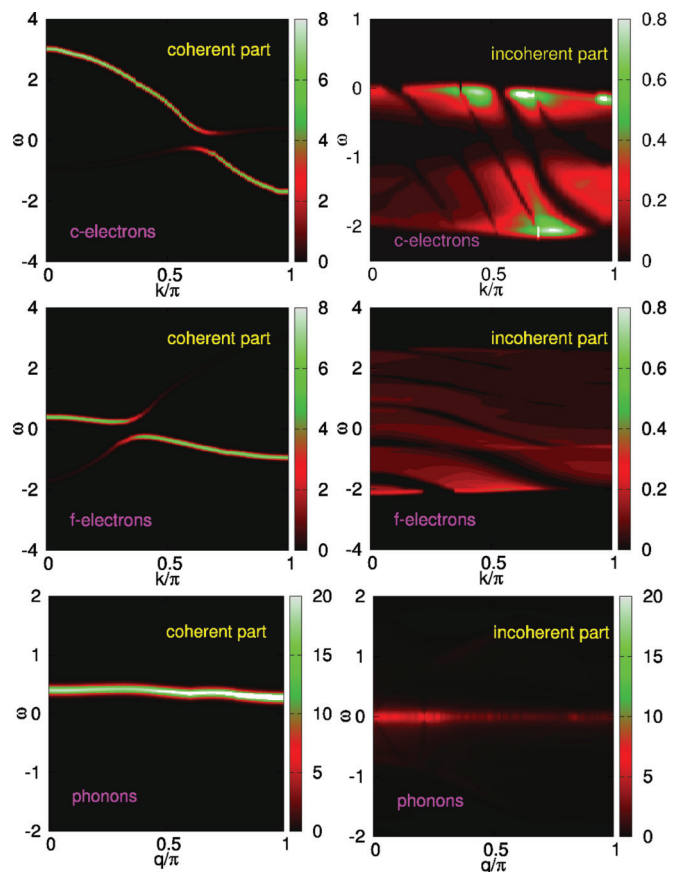


FIG. 8. (Color online) Intensity plots of the coherent (left-hand panels) and the incoherent (right-hand panels) parts of the c - and f -electron single-particle spectral functions and of the phonon spectral function. Note the different color coding of the coherent and incoherent parts of $A_k^{c,f}(\omega)$. We stress that also $A_k^c(\omega)$ has a finite incoherent part for $\omega > 0$ (as magnification would show), which only is noticeable in a small range above $\omega = 0$ however, because—among other factors—the renormalized f bandwidth is small. Results are given for $\omega_0 = 0.5$ and $g = 0.6$.

$A_k^c(\omega)$, $A_k^f(\omega)$, and $C_q(\omega)$ spectral functions separately. We choose as an example $g = 0.6$ and $\omega_0 = 0.5$; i.e., consider the system to be in the (adiabatic) EI or CDW regime (cf. Fig. 4). For these parameters the coherent signatures, given by the first terms in Eqs. (A49)–(A51) clearly dominate the spectra in each case (note that the intensity of the incoherent contributions is magnified by a factor of 10). They follow the renormalized dispersions E_k^c and E_k^f , possessing an excitation gap and a pronounced c - f -electron hybridization. Obviously the incoherent contribution of the c -electron spectrum is noticeable in the range of the f -electron band only (and vice versa) and will be enhanced if electron-phonon coupling increases. The phonon spectral function reveals that the signal at $\omega \simeq 0$ originates from the incoherent part of the spectrum. It acquires substantial spectral weight only if the renormalized quasiparticle bands will be “connected” by phonon absorption or emission processes which are significant at large g .

VI. SUMMARY

Applying a discrete version of the projective renormalization method to a two-band f - c -electron model with coupling to the lattice degrees of freedom we show that the exciton-phonon interaction can drive a semimetal to excitonic insulator transition at zero temperature in one dimension. The ground-state phase diagram containing semimetallic and excitonic insulator phases is derived. The excitonic condensate is accompanied by a charge-density wave and a finite lattice dimerization and is intimately connected with a developing f - c -electron coherence due to hybridization or coherence. At finite phonon frequency, this spontaneously symmetry-broken state does not appear until the interaction exceeds a finite critical coupling strength. The phase boundary determined by the projective renormalization method significantly deviates from the mean-field result in the intermediate exciton-phonon coupling and phonon frequency regime. The quantum phase transition shows up in the spectral quantities too: We notice the opening of a single-particle excitation gap in the photoemission spectrum, a substantial spectral weight transfer from the coherent to the incoherent part of the spectra, and a renormalization of the phonon mode, which becomes softened (hardened) as the transition point is reached in the adiabatic (nonadiabatic to antiadiabatic) regime. In this way our work points out the prominent role played by the lattice degrees of freedom establishing a charge-density wave in semimetallic systems with weak (indirect) band overlap and in mixed-valent semiconductors with band gaps comparable to the exciton binding energy, such as quasi-two-dimensional $1T$ -TiSe₂ and three-dimensional TmSe_{0.45}Te_{0.55}, respectively. For $1T$ -TiSe₂ it has been shown quite recently in the framework of a multiband extended Falicov-Kimball model that a purely electronic exciton pairing and condensation mechanism is insufficient to describe the observed (long-ranged) chiral charge order.²⁶ Hence the coupling to the phonons seems to be essential, and first mean-field results indicate that electron-hole Coulomb attraction and exciton-phonon coupling indeed support each other in establishing a charge-density wave state with small but finite lattice distortion. Essential electron correlation and all phonon fluctuation effects were neglected, however. Here we consider

a one-dimensional model, where quantum phonon fluctuations are exceedingly important and in general tend to suppress any long-range charge order or lattice dimerization, and show that a lattice coupling to electron-hole excitations of reasonable strength can nonetheless cause an excitonic instability. A future more complete theoretical discussion of the low-temperature properties of these material classes should definitely comprise the complex interplay of electron-phonon and electron-hole interactions beyond mean field, particularly in the vicinity of the semiconductor-semimetal transition.

ACKNOWLEDGMENTS

The authors would like to thank H. Beck, F. X. Bronold, S. Ejima, D. Ihle, S. Sykora, and B. Zenker for valuable discussions. This research is funded by Vietnam National Foundation for Science and Technology Development (NAFOSTED) under Grant No. 103.02-2012.52 and by Deutsche Forschungsgemeinschaft through SFB 652, B5.

APPENDIX A: PROJECTOR-BASED RENORMALIZATION METHOD

In this Appendix we demonstrate in detail how to solve Hamiltonian \mathcal{H} by means of the PRM. So far the PRM was successfully applied to the one-dimensional Holstein²⁷ and extended Falicov-Kimball¹² models and a number of other models. Its starting point is the decomposition of a many-particle Hamiltonian \mathcal{H} into an “unperturbed” part \mathcal{H}_0 and into a “perturbation” \mathcal{H}_1 , where the unperturbed part \mathcal{H}_0 is solvable. The perturbation is responsible for transitions between the eigenstates of \mathcal{H}_0 with nonvanishing transition energies $|E_0^n - E_0^m|$. Here E_0^n and E_0^m denote the energies of \mathcal{H}_0 between which the transitions take place. The basic idea of the PRM method is to integrate out the interaction \mathcal{H}_1 by a sequence of discrete unitary transformations.²⁰ Thereby, the PRM renormalization starts from the largest transition energy of the original Hamiltonian \mathcal{H}_0 , which will be called Λ , and proceeds in steps $\Delta\lambda$ to lower values of transition energies λ . For practical applications the unitary transformations are best done in small steps $\Delta\lambda$. Thereby, the evaluation in each step can be restricted to low orders in \mathcal{H}_1 . This procedure usually limits the validity of the approach to parameter values of \mathcal{H}_1 which are of the same magnitude as those of \mathcal{H}_0 . Every renormalization step is performed by means of a small unitary transformation, where all excitations between λ and $\lambda - \Delta\lambda$ are eliminated:

$$\mathcal{H}_{\lambda-\Delta\lambda} = e^{X_{\lambda,\Delta\lambda}} \mathcal{H}_\lambda e^{-X_{\lambda,\Delta\lambda}}. \quad (\text{A1})$$

Here, the operator $X_{\lambda,\Delta\lambda} = -X_{\lambda,\Delta\lambda}^\dagger$ is the generator of the unitary transformation for the small step. After each step both the unperturbed part of the Hamiltonian and the perturbation become renormalized and depend on the cutoff energy λ ; i.e., one arrives at a renormalized Hamiltonian $\mathcal{H}_\lambda = \mathcal{H}_{0,\lambda} + \mathcal{H}_{1,\lambda}$. Note that $\mathcal{H}_{1,\lambda}$ now only accounts for transitions with energies smaller than λ . Proceeding the renormalization stepwise up to zero transition energies $\lambda = 0$ all transitions with energies different from zero have been integrated out. Thus, finally one arrives at a renormalized Hamiltonian $\mathcal{H}_{\lambda=0}$, which is diagonal

or at least quasi-diagonal, since all transitions from \mathcal{H}_1 have been used up.

1. Hamiltonian \mathcal{H}_λ

Assuming that all transitions with energies larger than λ are already integrated out, an appropriate *ansatz* in the present case for the transformed Hamiltonian \mathcal{H}_λ reads $\mathcal{H}_\lambda = \mathcal{H}_{0,\lambda} + \mathcal{H}_{1,\lambda}$, with

$$\begin{aligned} \mathcal{H}_{0,\lambda} &= \sum_{\mathbf{k}} \varepsilon_{\mathbf{k},\lambda}^f f_{\mathbf{k}}^\dagger f_{\mathbf{k}} + \sum_{\mathbf{k}} \varepsilon_{\mathbf{k},\lambda}^c c_{\mathbf{k}}^\dagger c_{\mathbf{k}} + \sum_{\mathbf{q}} \omega_{\mathbf{q},\lambda} B_{\mathbf{q},\lambda}^\dagger B_{\mathbf{q},\lambda} \\ &\quad + \Delta_\lambda \sum_{\mathbf{k}} (c_{\mathbf{k}+\mathbf{Q}}^\dagger f_{\mathbf{k}} + f_{\mathbf{k}}^\dagger c_{\mathbf{k}+\mathbf{Q}}), \end{aligned} \quad (\text{A2})$$

$$\mathcal{H}_{1,\lambda} = \frac{g}{\sqrt{N}} \sum_{\mathbf{k}\mathbf{q}} \mathbf{P}_\lambda [\delta(c_{\mathbf{k}+\mathbf{q}}^\dagger f_{\mathbf{k}}) \delta(B_{-\mathbf{q},\lambda}^\dagger + B_{\mathbf{q},\lambda}) + \text{H.c.}]. \quad (\text{A3})$$

The parameters of $\mathcal{H}_{0,\lambda}$ depend on the cutoff λ . Also, the phonon energy has acquired an additional \mathbf{q} dependence. Moreover, we have introduced λ -dependent phonon operators

$$B_{\mathbf{q},\lambda}^\dagger = b_{\mathbf{q}}^\dagger + \frac{\sqrt{N}h_\lambda}{\omega_{\mathbf{Q},\lambda}} \delta_{\mathbf{q},\mathbf{Q}}, \quad (\text{A4})$$

in a slight generalization of the former definition Eq. (12). Finally, the quantity \mathbf{P}_λ in Eq. (A3) is a generalized projector, which projects on all transitions (with respect to $\mathcal{H}_{0,\lambda}$) with energies smaller than λ . Note that the coupling strength g of $\mathcal{H}_{1,\lambda}$ remains λ independent as a consequence of the present restriction to renormalization contributions up to order g^2 .

Next, \mathbf{P}_λ has to be applied to the operators $\delta(c_{\mathbf{k}+\mathbf{q}}^\dagger f_{\mathbf{k}}) \delta(B_{-\mathbf{q},\lambda}^\dagger + B_{\mathbf{q},\lambda})$ in $\mathcal{H}_{1,\lambda}$, which requires the decomposition of the operators in the squared brackets into dynamical eigenmodes of $\mathcal{H}_{0,\lambda}$. One may show that one can use for $\mathcal{H}_{1,\lambda}$

$$\begin{aligned} \mathcal{H}_{1,\lambda} &= \frac{g}{\sqrt{N}} \sum_{\mathbf{k}\mathbf{q}} [\Theta_{\mathbf{k}\mathbf{q},\lambda}^+ (\delta(c_{\mathbf{k}+\mathbf{q}}^\dagger f_{\mathbf{k}}) \delta B_{-\mathbf{q},\lambda}^\dagger + \text{H.c.}) \\ &\quad + \Theta_{\mathbf{k}\mathbf{q},\lambda}^- (\delta(c_{\mathbf{k}+\mathbf{q}}^\dagger f_{\mathbf{k}}) \delta B_{\mathbf{q},\lambda} + \text{H.c.})] \end{aligned} \quad (\text{A5})$$

as long as one is only interested in renormalization equations up to linear order in the order parameters. In Eq. (A5) we have introduced two Θ functions

$$\Theta_{\mathbf{k}\mathbf{q},\lambda}^\pm = \Theta(\lambda - |\varepsilon_{\mathbf{k}+\mathbf{q},\lambda}^c - \varepsilon_{\mathbf{k},\lambda}^f \pm \omega_{\mp\mathbf{q},\lambda}|), \quad (\text{A6})$$

which restrict transitions to excitation energies smaller than λ .

One can also construct the generator $X_{\lambda,\Delta\lambda}$ of the unitary transformation Eq. (A1) for the transformation from cutoff λ to $\lambda - \Delta\lambda$. According to Ref. 20 the lowest order for $X_{\lambda,\Delta\lambda}$ is given by

$$X_{\lambda,\Delta\lambda} = \frac{1}{\mathbf{L}_{0,\lambda}} \mathbf{Q}_{\lambda-\Delta\lambda} \mathcal{H}_{1,\lambda}. \quad (\text{A7})$$

Here $\mathbf{L}_{0,\lambda}$ is the Liouville operator of the unperturbed Hamiltonian $\mathcal{H}_{0,\lambda}$, which is defined by $\mathbf{L}_{0,\lambda} \mathcal{A} = [\mathcal{H}_{0,\lambda}, \mathcal{A}]$ for any operator quantity \mathcal{A} , and $\mathbf{Q}_{\lambda-\Delta\lambda} = 1 - \mathbf{P}_{\lambda-\Delta\lambda}$ is the complement projector to $\mathbf{P}_{\lambda-\Delta\lambda}$. It projects on all transition operators with excitation energies larger than $\lambda - \Delta\lambda$. With

Eqs. (A2) and (A5) one finds

$$\begin{aligned} X_{\lambda,\Delta\lambda} &= \frac{g}{\sqrt{N}} \sum_{\mathbf{k}\mathbf{q}} [A_{\mathbf{k}\mathbf{q}}^+(\lambda, \Delta\lambda) (\delta(c_{\mathbf{k}+\mathbf{q}}^\dagger f_{\mathbf{k}}) \delta B_{-\mathbf{q},\lambda}^\dagger - \text{H.c.}) \\ &\quad + A_{\mathbf{k}\mathbf{q}}^-(\lambda, \Delta\lambda) (\delta(c_{\mathbf{k}+\mathbf{q}}^\dagger f_{\mathbf{k}}) \delta B_{\mathbf{q},\lambda} - \text{H.c.})], \end{aligned} \quad (\text{A8})$$

where the prefactors are given by

$$A_{\mathbf{k}\mathbf{q}}^\pm(\lambda, \Delta\lambda) = \frac{\Theta_{\mathbf{k}\mathbf{q},\lambda}^\pm (1 - \Theta_{\mathbf{k}\mathbf{q},\lambda-\Delta\lambda}^\pm)}{\varepsilon_{\mathbf{k}+\mathbf{q},\lambda}^c - \varepsilon_{\mathbf{k},\lambda}^f \pm \omega_{\mp\mathbf{q},\lambda}}. \quad (\text{A9})$$

Here the products of the two Θ functions in $A_{\mathbf{k}\mathbf{q}}^\pm(\lambda, \Delta\lambda)$ assure that only excitations between λ and $\lambda - \Delta\lambda$ are eliminated by the unitary transformation Eq. (A1). Also note that the Liouville operator $\mathbf{L}_{0,\lambda}$ in $X_{\lambda,\Delta\lambda}$ (and the projector \mathbf{P}_λ in $\mathcal{H}_{1,\lambda}$) in principle should have been defined with respect to the full unperturbed Hamiltonian $\mathcal{H}_{0,\lambda}$ of Eq. (A2) and not by leaving out the last term $\propto \Delta_\lambda$. However, inclusion of this term would only give small higher-order corrections to Δ_λ .

2. Renormalization equations

The λ dependence of the parameters of \mathcal{H}_λ are found from transformation Eq. (A1). For small enough width $\Delta\lambda$ of the transformation steps, the expansion of Eq. (A1) in g can be limited to $\mathcal{O}(g^2)$ terms. One obtains

$$\begin{aligned} \mathcal{H}_{\lambda-\Delta\lambda} &= \mathcal{H}_{0,\lambda} + \mathbf{P}_{\lambda-\Delta\lambda} \mathcal{H}_{1,\lambda} + [X_{\lambda,\Delta\lambda}, \mathcal{H}_{1,\lambda}] \\ &\quad - \frac{1}{2} [X_{\lambda,\Delta\lambda}, \mathbf{Q}_{\lambda-\Delta\lambda} \mathcal{H}_{1,\lambda}] + \dots, \end{aligned} \quad (\text{A10})$$

where Eq. (A7) has been used. Renormalization contributions to $\mathcal{H}_{\lambda-\Delta\lambda}$ arise from the last two commutators, which have to be evaluated explicitly. The result must be compared with the generic form [Eqs. (A2) and (A3)] of \mathcal{H}_λ (with λ replaced by $\lambda - \Delta\lambda$) when it is written in terms of the original λ -independent variables $c_{\mathbf{k}}^\dagger$, $f_{\mathbf{k}}^\dagger$, and $b_{\mathbf{q}}^\dagger$. This leads to the following renormalization equations for the parameters of $\mathcal{H}_{0,\lambda}$:

$$\begin{aligned} \varepsilon_{\mathbf{k},\lambda-\Delta\lambda}^c - \varepsilon_{\mathbf{k},\lambda}^c &= \frac{2g^2}{N} \sum_{\mathbf{q}} (A_{\mathbf{k}-\mathbf{q},\mathbf{q}}^+(\lambda, \Delta\lambda) (n_{-\mathbf{q}}^B + n_{\mathbf{k}-\mathbf{q}}^f) \\ &\quad + A_{\mathbf{k}-\mathbf{q},\mathbf{q}}^-(\lambda, \Delta\lambda) (1 + n_{\mathbf{q}}^B - n_{\mathbf{k}-\mathbf{q}}^f)), \end{aligned} \quad (\text{A11})$$

$$\begin{aligned} \varepsilon_{\mathbf{k},\lambda-\Delta\lambda}^f - \varepsilon_{\mathbf{k},\lambda}^f &= -\frac{2g^2}{N} \sum_{\mathbf{q}} (A_{\mathbf{k}\mathbf{q}}^+(\lambda, \Delta\lambda) (1 - n_{\mathbf{k}+\mathbf{q}}^c + n_{-\mathbf{q}}^B) \\ &\quad + A_{\mathbf{k}\mathbf{q}}^-(\lambda, \Delta\lambda) (n_{\mathbf{k}+\mathbf{q}}^c + n_{-\mathbf{q}}^B)), \end{aligned} \quad (\text{A12})$$

and

$$\begin{aligned} \omega_{\mathbf{q},\lambda-\Delta\lambda} - \omega_{\mathbf{q},\lambda} &= -\frac{2g^2}{N} \sum_{\mathbf{k}} [A_{\mathbf{k},-\mathbf{q}}^+(\lambda, \Delta\lambda) (n_{\mathbf{k}}^f - n_{\mathbf{k}-\mathbf{q}}^c) \\ &\quad + A_{\mathbf{k},\mathbf{q}}^-(\lambda, \Delta\lambda) (n_{\mathbf{k}}^f - n_{\mathbf{k}+\mathbf{q}}^c)], \end{aligned} \quad (\text{A13})$$

$$\begin{aligned} h_{\lambda-\Delta\lambda} - h_\lambda &= -\frac{g^2}{N\sqrt{N}} \sum_{\mathbf{k}} [A_{\mathbf{k},-\mathbf{Q}}^+(\lambda, \Delta\lambda) (n_{\mathbf{k}-\mathbf{Q}}^c - n_{\mathbf{k}}^f) \\ &\quad + A_{\mathbf{k},\mathbf{Q}}^-(\lambda, \Delta\lambda) (n_{\mathbf{k}+\mathbf{Q}}^c - n_{\mathbf{k}}^f)] (\langle b_{\mathbf{Q}} \rangle + \langle b_{\mathbf{Q}}^\dagger \rangle), \end{aligned} \quad (\text{A14})$$

$$\Delta_{\lambda-\Delta\lambda} - \Delta_\lambda \simeq 0. \quad (\text{A15})$$

The quantities $n_{\mathbf{k}}^c$, $n_{\mathbf{k}}^f$, and $n_{\mathbf{q}}^B$ are occupation numbers for electrons and phonons,

$$n_{\mathbf{k}}^c = \langle c_{\mathbf{k}}^\dagger c_{\mathbf{k}} \rangle, \quad n_{\mathbf{k}}^f = \langle f_{\mathbf{k}}^\dagger f_{\mathbf{k}} \rangle, \quad (\text{A16})$$

$$n_{\mathbf{q}}^B = \langle \delta B_{\mathbf{q},\lambda}^\dagger \delta B_{\mathbf{q},\lambda} \rangle = \langle \delta b_{\mathbf{q}}^\dagger \delta b_{\mathbf{q}} \rangle, \quad (\text{A17})$$

and have to be evaluated separately. Note that also $n_{\mathbf{q}}^B$ is λ independent, which was already used in the renormalization equations. For the numerical solution in Sec. V the initial parameter values at $\lambda = \Lambda$ are needed, which are those of the original Hamiltonian \mathcal{H} :

$$\varepsilon_{\mathbf{k},\Lambda}^f = \varepsilon_{\mathbf{k}}^f, \quad \varepsilon_{\mathbf{k},\Lambda}^c = \varepsilon_{\mathbf{k}}^c, \quad \omega_{\mathbf{q},\Lambda} = \omega_0, \quad (\text{A18})$$

and

$$h_\Lambda = h = 0^+, \quad \Delta_\Lambda = \Delta = 0^+. \quad (\text{A19})$$

Supposing the expectation values in Eqs. (A11)–(A15) are already known, the renormalization equations can be integrated between $\lambda = \Lambda$ and 0. In this way, we obtain the fully renormalized Hamiltonian $\tilde{\mathcal{H}} := \mathcal{H}_{\lambda=0} = \mathcal{H}_{0,\lambda=0}$, as was already stated in Eq. (29):

$$\begin{aligned} \tilde{\mathcal{H}} = & \sum_{\mathbf{k}} \tilde{\varepsilon}_{\mathbf{k}}^f f_{\mathbf{k}}^\dagger f_{\mathbf{k}} + \sum_{\mathbf{k}} \tilde{\varepsilon}_{\mathbf{k}}^c c_{\mathbf{k}}^\dagger c_{\mathbf{k}} + \sum_{\mathbf{q}} \tilde{\omega}_{\mathbf{q}} b_{\mathbf{q}}^\dagger b_{\mathbf{q}} \\ & + \tilde{\Delta} \sum_{\mathbf{k}} (c_{\mathbf{k}+\mathbf{Q}}^\dagger f_{\mathbf{k}} + \text{H.c.}) + \sqrt{N} \tilde{h} (b_{-\mathbf{Q}}^\dagger + b_{-\mathbf{Q}}). \end{aligned} \quad (\text{A20})$$

The tilde symbols denote the fully renormalized quantities at $\lambda = 0$. All excitations from $\mathcal{H}_{1,\lambda}$ with nonzero energies have been eliminated. They give rise to the renormalization of $\mathcal{H}_{0,\lambda}$. Note that the order parameter Δ remains unrenormalized, i.e., $\tilde{\Delta} = \Delta$, due to renormalization equation Eq. (A15).

Finally, Eq. (A20) can be expressed in terms of the renormalized boson operator $\tilde{B}_{\mathbf{q}}^\dagger = b_{\mathbf{q}}^\dagger + (\sqrt{N}\tilde{h}/\tilde{\omega}_{\mathbf{q}})\delta_{\mathbf{q},\mathbf{Q}}$, which gives

$$\begin{aligned} \tilde{\mathcal{H}} = & \sum_{\mathbf{k}} \tilde{\varepsilon}_{\mathbf{k}}^f f_{\mathbf{k}}^\dagger f_{\mathbf{k}} + \sum_{\mathbf{k}} \tilde{\varepsilon}_{\mathbf{k}}^c c_{\mathbf{k}}^\dagger c_{\mathbf{k}} + \sum_{\mathbf{q}} \tilde{\omega}_{\mathbf{q}} \tilde{B}_{\mathbf{q}}^\dagger \tilde{B}_{\mathbf{q}} \\ & + \tilde{\Delta} \sum_{\mathbf{k}} (c_{\mathbf{k}+\mathbf{Q}}^\dagger f_{\mathbf{k}} + \text{H.c.}). \end{aligned} \quad (\text{A21})$$

As in the unrenormalized case, the electronic part of $\tilde{\mathcal{H}}$ will be diagonalized by a Bogoliubov transformation, which gives

$$\begin{aligned} \tilde{\mathcal{H}} = & \sum_{\mathbf{k}} \tilde{E}_{\mathbf{k}}^{(1)} C_{1,\mathbf{k}}^\dagger C_{1,\mathbf{k}} + \sum_{\mathbf{k}} \tilde{E}_{\mathbf{k}}^{(2)} C_{2,\mathbf{k}}^\dagger C_{2,\mathbf{k}} \\ & + \sum_{\mathbf{q}} \tilde{\omega}_{\mathbf{q}} \tilde{B}_{\mathbf{q}}^\dagger \tilde{B}_{\mathbf{q}} + \text{const.} \end{aligned} \quad (\text{A22})$$

In result Eq. (A22) the electronic quasiparticle energies $\tilde{E}_{\mathbf{k}}^{(1,2)}$ and also the quasiparticle modes $C_{1,\mathbf{k}}^{(\dagger)}$ and $C_{2,\mathbf{k}}^{(\dagger)}$ are now renormalized quantities. They are defined by the former equations Eqs. (17)–(22) when the unrenormalized energies $\varepsilon_{\mathbf{k}}^c$ and $\varepsilon_{\mathbf{k}}^f$ are replaced by the renormalized energies $\tilde{\varepsilon}_{\mathbf{k}}^c$ and $\tilde{\varepsilon}_{\mathbf{k}}^f$. Note that the quadratic form of Eq. (A22) allows us to compute any expectation value formed with $\tilde{\mathcal{H}}$.

3. Expectation values

Next, expectation values $\langle \mathcal{A} \rangle$, formed with the full \mathcal{H} , have to be evaluated in the framework of the PRM. As

already stated in Sec. IV, they can be found by exploiting the unitary invariance of operator expressions below a trace. Employing the same unitary transformation to \mathcal{A} as before for the Hamiltonian,²⁰ one finds $\langle \mathcal{A} \rangle = \langle \mathcal{A}(\lambda) \rangle_{\mathcal{H}_\lambda} = \langle \tilde{\mathcal{A}} \rangle_{\tilde{\mathcal{H}}}$. Here $\mathcal{A}(\lambda) = e^{X_\lambda} \mathcal{A} e^{-X_\lambda}$ and $\tilde{\mathcal{A}} = \mathcal{A}(\lambda = 0)$. X_λ is the generator for the unitary transformation between cutoff Λ and λ . To find the expectation values of Eqs. (A16) and (A17) one best starts from an *ansatz* for the single fermion operators $c_{\mathbf{k}}^\dagger(\lambda) = e^{X_\lambda} c_{\mathbf{k}}^\dagger e^{-X_\lambda}$ and $f_{\mathbf{k}}^\dagger(\lambda) = e^{X_\lambda} f_{\mathbf{k}}^\dagger e^{-X_\lambda}$ and the phonon operator $b_{\mathbf{q}}^\dagger(\lambda) = e^{X_\lambda} b_{\mathbf{q}}^\dagger e^{-X_\lambda}$, at cutoff λ . In second order in the electron-phonon interaction they are chosen as

$$\begin{aligned} c_{\mathbf{k}}^\dagger(\lambda) = & x_{\mathbf{k},\lambda} c_{\mathbf{k}}^\dagger + \frac{1}{\sqrt{N}} \sum_{\mathbf{q}} t_{\mathbf{k}-\mathbf{q},\mathbf{q},\lambda}^+ f_{\mathbf{k}-\mathbf{q}}^\dagger \delta(B_{-\mathbf{q},\lambda}) \\ & + \frac{1}{\sqrt{N}} \sum_{\mathbf{q}} t_{\mathbf{k}-\mathbf{q},\mathbf{q},\lambda}^- f_{\mathbf{k}-\mathbf{q}}^\dagger \delta(B_{\mathbf{q},\lambda}), \end{aligned} \quad (\text{A23})$$

$$\begin{aligned} f_{\mathbf{k}}^\dagger(\lambda) = & y_{\mathbf{k},\lambda} f_{\mathbf{k}}^\dagger + \frac{1}{\sqrt{N}} \sum_{\mathbf{q}} u_{\mathbf{k}\mathbf{q},\lambda}^+ c_{\mathbf{k}+\mathbf{q}}^\dagger \delta(B_{-\mathbf{q},\lambda}) \\ & + \frac{1}{\sqrt{N}} \sum_{\mathbf{q}} u_{\mathbf{k}\mathbf{q},\lambda}^- c_{\mathbf{k}+\mathbf{q}}^\dagger \delta(B_{\mathbf{q},\lambda}), \end{aligned} \quad (\text{A24})$$

$$\begin{aligned} b_{\mathbf{q}}^\dagger(\lambda) = & z_{\mathbf{q},\lambda} b_{\mathbf{q}}^\dagger + \frac{1}{\sqrt{N}} \sum_{\mathbf{k}} v_{\mathbf{k},-\mathbf{q},\lambda}^+ \delta(f_{\mathbf{k}}^\dagger c_{\mathbf{k}-\mathbf{q}}) \\ & + \frac{1}{\sqrt{N}} \sum_{\mathbf{k}} v_{\mathbf{k}\mathbf{q},\lambda}^- \delta(c_{\mathbf{k}+\mathbf{q}}^\dagger f_{\mathbf{k}}). \end{aligned} \quad (\text{A25})$$

In analogy to the renormalization equations for the parameters of \mathcal{H}_λ , one first derives the following set of renormalization equations for the coefficients $t_{\mathbf{k}-\mathbf{q},\mathbf{q},\lambda}^\pm$, $u_{\mathbf{k}\mathbf{q},\lambda}^\pm$, and $v_{\mathbf{k},\mp\mathbf{q},\lambda}^\pm$:

$$t_{\mathbf{k}-\mathbf{q},\mathbf{q},\lambda-\Delta\lambda}^\pm = t_{\mathbf{k}-\mathbf{q},\mathbf{q},\lambda}^\pm - g x_{\mathbf{k},\lambda} A_{\mathbf{k}-\mathbf{q},\mathbf{q}}^\pm(\lambda, \Delta\lambda), \quad (\text{A26})$$

$$u_{\mathbf{k}\mathbf{q},\lambda-\Delta\lambda}^\pm = u_{\mathbf{k}\mathbf{q},\lambda}^\pm + g y_{\mathbf{k},\lambda} A_{\mathbf{k}\mathbf{q}}^\pm(\lambda, \Delta\lambda), \quad (\text{A27})$$

$$v_{\mathbf{k},\mp\mathbf{q},\lambda-\Delta\lambda}^\pm = v_{\mathbf{k},\mp\mathbf{q},\lambda}^\pm - g z_{\mathbf{q},\lambda} A_{\mathbf{k},\mp\mathbf{q}}^\pm(\lambda, \Delta\lambda). \quad (\text{A28})$$

Using the anticommutation relations for fermion operators and the commutation relations for boson operators—as, for instance, $[c_{\mathbf{k}}^\dagger(\lambda), c_{\mathbf{k}}(\lambda)]_+ = 1$, valid for any λ —one arrives at

$$\begin{aligned} |x_{\mathbf{k},\lambda}|^2 = & 1 - \frac{1}{N} \sum_{\mathbf{q}} [|t_{\mathbf{k}-\mathbf{q},\mathbf{q},\lambda}^+|^2 (n_{-\mathbf{q},\lambda}^B + n_{\mathbf{k}-\mathbf{q}}^f) \\ & + |t_{\mathbf{k}-\mathbf{q},\mathbf{q},\lambda}^-|^2 (1 + n_{\mathbf{q},\lambda}^B - n_{\mathbf{k}-\mathbf{q}}^f)], \end{aligned} \quad (\text{A29})$$

$$\begin{aligned} |y_{\mathbf{k},\lambda}|^2 = & 1 - \frac{1}{N} \sum_{\mathbf{q}} [|u_{\mathbf{k}\mathbf{q},\lambda}^+|^2 (n_{-\mathbf{q},\lambda}^B + 1 - n_{\mathbf{k}+\mathbf{q}}^c) \\ & + |u_{\mathbf{k}\mathbf{q},\lambda}^-|^2 (n_{\mathbf{q},\lambda}^B + n_{\mathbf{k}+\mathbf{q}}^c)], \end{aligned} \quad (\text{A30})$$

$$\begin{aligned} |z_{\mathbf{q},\lambda}|^2 = & 1 - \frac{1}{N} \sum_{\mathbf{k}} [|v_{\mathbf{k},-\mathbf{q},\lambda}^+|^2 (n_{\mathbf{k}-\mathbf{q}}^c - n_{\mathbf{k}}^f) \\ & + |v_{\mathbf{k}\mathbf{q},\lambda}^-|^2 (n_{\mathbf{k}}^f - n_{\mathbf{k}+\mathbf{q}}^c)]. \end{aligned} \quad (\text{A31})$$

Note that Eqs. (A26)–(A28), together with the new set Eqs. (A29)–(A31), taken at $\lambda \rightarrow \lambda - \Delta\lambda$, represent a complete set of renormalization equations for all λ -dependent coefficients in Eqs. (A23)–(A25). They combine the parameter values at λ with those at $\lambda - \Delta\lambda$. By integrating the full set

between $\lambda = \Lambda$, with initial parameter values

$$\{x_{\mathbf{k}\Lambda}, y_{\mathbf{k}\Lambda}, z_{\mathbf{k}\Lambda}\} = 1, \quad \{u_{\mathbf{k}\mathbf{q},\Lambda}^\pm, v_{\mathbf{k}\mathbf{q},\Lambda}^\pm\} = 0, \quad (\text{A32})$$

and $\lambda = 0$, one is led to the fully renormalized one-particle operators:

$$\begin{aligned} \tilde{c}_{\mathbf{k}}^\dagger &= \tilde{x}_{\mathbf{k}} c_{\mathbf{k}}^\dagger + \frac{1}{\sqrt{N}} \sum_{\mathbf{q}} \tilde{t}_{\mathbf{k}-\mathbf{q},\mathbf{q}}^+ f_{\mathbf{k}-\mathbf{q}}^\dagger \delta(\tilde{B}_{-\mathbf{q}}) \\ &+ \frac{1}{\sqrt{N}} \sum_{\mathbf{q}} \tilde{t}_{\mathbf{k}-\mathbf{q},\mathbf{q}}^- f_{\mathbf{k}-\mathbf{q}}^\dagger \delta(\tilde{B}_{\mathbf{q}}^\dagger), \end{aligned} \quad (\text{A33})$$

$$\begin{aligned} \tilde{f}_{\mathbf{k}}^\dagger &= \tilde{y}_{\mathbf{k}} f_{\mathbf{k}}^\dagger + \frac{1}{\sqrt{N}} \sum_{\mathbf{q}} \tilde{u}_{\mathbf{k}\mathbf{q}}^+ c_{\mathbf{k}+\mathbf{q}}^\dagger \delta(\tilde{B}_{-\mathbf{q}}^\dagger) \\ &+ \frac{1}{\sqrt{N}} \sum_{\mathbf{q}} \tilde{u}_{\mathbf{k}\mathbf{q}}^- c_{\mathbf{k}+\mathbf{q}}^\dagger \delta(\tilde{B}_{\mathbf{q}}), \end{aligned} \quad (\text{A34})$$

$$\begin{aligned} \tilde{b}_{\mathbf{q}}^\dagger &= \tilde{z}_{\mathbf{q}} b_{\mathbf{q}}^\dagger + \frac{1}{\sqrt{N}} \sum_{\mathbf{k}} \tilde{v}_{\mathbf{k},-\mathbf{q}}^+ \delta(f_{\mathbf{k}}^\dagger c_{\mathbf{k}-\mathbf{q}}) \\ &+ \frac{1}{\sqrt{N}} \sum_{\mathbf{k}} \tilde{v}_{\mathbf{k}\mathbf{q}}^- \delta(c_{\mathbf{k}+\mathbf{q}}^\dagger f_{\mathbf{k}}). \end{aligned} \quad (\text{A35})$$

As before, the tilde symbols denote fully renormalized quantities. With Eqs. (A33)–(A35) the expectation values Eqs. (A16) and (A17) can be evaluated. The expectation values for fermion operators read up to order $\mathcal{O}(g_k^2)$

$$\begin{aligned} n_{\mathbf{k}}^c &= |\tilde{x}_{\mathbf{k}}|^2 \tilde{n}_{\mathbf{k}}^c + \frac{1}{N} \sum_{\mathbf{q}} [|\tilde{t}_{\mathbf{k}-\mathbf{q},\mathbf{q}}^+|^2 \tilde{n}_{\mathbf{k}-\mathbf{q}}^f (1 + \tilde{n}_{-\mathbf{q}}^B) \\ &+ |\tilde{t}_{\mathbf{k}-\mathbf{q},\mathbf{q}}^-|^2 \tilde{n}_{\mathbf{k}-\mathbf{q}}^f \tilde{n}_{\mathbf{q}}^B], \end{aligned} \quad (\text{A36})$$

$$\begin{aligned} n_{\mathbf{k}}^f &= |\tilde{y}_{\mathbf{k}}|^2 \tilde{n}_{\mathbf{k}}^f + \frac{1}{N} \sum_{\mathbf{q}} [|\tilde{u}_{\mathbf{k}\mathbf{q}}^+|^2 \tilde{n}_{\mathbf{k}+\mathbf{q}}^c \tilde{n}_{-\mathbf{q}}^B \\ &+ |\tilde{u}_{\mathbf{k}\mathbf{q}}^-|^2 \tilde{n}_{\mathbf{k}+\mathbf{q}}^c (1 + \tilde{n}_{\mathbf{q}}^B)], \end{aligned} \quad (\text{A37})$$

$$\begin{aligned} d_{\mathbf{k}} &= \tilde{x}_{\mathbf{k}+\mathbf{Q}} \tilde{y}_{\mathbf{k}} \langle c_{\mathbf{k}+\mathbf{Q}}^\dagger f_{\mathbf{k}} \rangle_{\tilde{\mathcal{H}}} \\ &+ \frac{1}{N} \sum_{\mathbf{q}} [\tilde{t}_{\mathbf{k}+\mathbf{Q}-\mathbf{q},\mathbf{q}}^+ \tilde{u}_{\mathbf{k},-\mathbf{q}}^- \langle f_{\mathbf{k}+\mathbf{Q}-\mathbf{q}}^\dagger c_{\mathbf{k}-\mathbf{q}} \rangle_{\tilde{\mathcal{H}}} (1 - \tilde{n}_{-\mathbf{q}}^B) \\ &+ \tilde{t}_{\mathbf{k}+\mathbf{Q}-\mathbf{q},\mathbf{q}}^- \tilde{u}_{\mathbf{k},-\mathbf{q}}^+ \langle f_{\mathbf{k}+\mathbf{Q}-\mathbf{q}}^\dagger c_{\mathbf{k}-\mathbf{q}} \rangle_{\tilde{\mathcal{H}}} \tilde{n}_{\mathbf{q}}^B]. \end{aligned} \quad (\text{A38})$$

Here $d_{\mathbf{k}} = \langle c_{\mathbf{k}+\mathbf{Q}}^\dagger f_{\mathbf{k}} \rangle$ [Eq. (4)] is an additional quantity, which acts as an excitonic order parameter. The expectation values on the right-hand sides of Eqs. (A39)–(A41) are formed with $\tilde{\mathcal{H}}$ and can be evaluated, i.e.,

$$\tilde{n}_{\mathbf{k}+\mathbf{Q}}^c = \langle c_{\mathbf{k}+\mathbf{Q}}^\dagger c_{\mathbf{k}+\mathbf{Q}} \rangle_{\tilde{\mathcal{H}}} = \xi_{\mathbf{k}}^2 f^F(\tilde{E}_{\mathbf{k}}^1) + \eta_{\mathbf{k}}^2 f^F(\tilde{E}_{\mathbf{k}}^2), \quad (\text{A39})$$

$$\tilde{n}_{\mathbf{k}}^f = \langle f_{\mathbf{k}}^\dagger f_{\mathbf{k}} \rangle_{\tilde{\mathcal{H}}} = \eta_{\mathbf{k}}^2 f^F(\tilde{E}_{\mathbf{k}}^1) + \xi_{\mathbf{k}}^2 f^F(\tilde{E}_{\mathbf{k}}^2), \quad (\text{A40})$$

$$\langle c_{\mathbf{k}+\mathbf{Q}}^\dagger f_{\mathbf{k}} \rangle_{\tilde{\mathcal{H}}} = -[f^F(\tilde{E}_{\mathbf{k}}^1) - f^F(\tilde{E}_{\mathbf{k}}^2)] \text{sgn}(\tilde{\epsilon}_{\mathbf{k}}^f - \tilde{\epsilon}_{\mathbf{k}+\mathbf{Q}}^c) \frac{\tilde{\Delta}}{W_{\mathbf{k}}}. \quad (\text{A41})$$

Here the prefactors $\xi_{\mathbf{k}}$ and $\eta_{\mathbf{k}}$ are the coefficients from the Bogoliubov transformation, used in Eq. (A22). As mentioned, they are defined by Eqs. (20) and (21), when the unrenormalized one-particle energies are replaced by the renormalized ones.

The bosonic expectation value Eq. (A17) is given by

$$n_{\mathbf{q}}^B = \langle \delta b_{\mathbf{q}}^\dagger \delta b_{\mathbf{q}} \rangle = \langle b_{\mathbf{q}}^\dagger b_{\mathbf{q}} \rangle - \langle b_{\mathbf{q}}^\dagger \rangle \langle b_{\mathbf{q}} \rangle \delta_{\mathbf{q}=\mathbf{Q}}, \quad (\text{A42})$$

where

$$\begin{aligned} \langle b_{\mathbf{q}}^\dagger b_{\mathbf{q}} \rangle &= |\tilde{z}_{\mathbf{q}}|^2 \tilde{n}_{\mathbf{q}}^b + \frac{1}{N} \sum_{\mathbf{k}} [|\tilde{v}_{\mathbf{k},-\mathbf{q}}^+|^2 \tilde{n}_{\mathbf{k}}^f (1 - \tilde{n}_{\mathbf{k}-\mathbf{q}}^c) \\ &+ |\tilde{v}_{\mathbf{k}\mathbf{q}}^-|^2 \tilde{n}_{\mathbf{k}+\mathbf{q}}^c (1 - \tilde{n}_{\mathbf{k}}^f)], \end{aligned} \quad (\text{A43})$$

$$\langle b_{\mathbf{q}}^\dagger \rangle \simeq \tilde{z}_{\mathbf{q}} \langle b_{\mathbf{q}}^\dagger \rangle_{\tilde{\mathcal{H}}}. \quad (\text{A44})$$

We emphasize that in $\langle b_{\mathbf{q}}^\dagger \rangle$ smaller contributions from Eq. (A35) have been neglected. Using Eq. (A21) the expectation values $\tilde{n}_{\mathbf{q}}^b = \langle b_{\mathbf{q}}^\dagger b_{\mathbf{q}} \rangle_{\tilde{\mathcal{H}}}$ and $\langle b_{\mathbf{q}}^\dagger \rangle_{\tilde{\mathcal{H}}}$ on the right-hand sides become

$$\begin{aligned} \tilde{n}_{\mathbf{q}}^b &= \langle B_{\mathbf{q}}^\dagger B_{\mathbf{q}} \rangle_{\tilde{\mathcal{H}}} - \frac{\sqrt{N} \tilde{h}}{\tilde{\omega}_{\mathbf{q}}} \langle B_{\mathbf{q}}^\dagger + B_{\mathbf{q}} \rangle_{\tilde{\mathcal{H}}} \delta_{\mathbf{q},\mathbf{Q}} + \frac{N \tilde{h}^2}{\tilde{\omega}_{\mathbf{q}}^2} \delta_{\mathbf{q},\mathbf{Q}} \\ &= f^B(\tilde{\omega}_{\mathbf{q}}) + \frac{N \tilde{h}^2}{\tilde{\omega}_{\mathbf{q}}^2} \delta_{\mathbf{q},\mathbf{Q}} \end{aligned} \quad (\text{A45})$$

and

$$\langle b_{\mathbf{q}}^\dagger \rangle_{\tilde{\mathcal{H}}} = \left[\langle B_{\mathbf{q}}^\dagger \rangle_{\tilde{\mathcal{H}}} - \frac{\sqrt{N} \tilde{h}}{\tilde{\omega}_{\mathbf{q}}} \right] \delta_{\mathbf{q},\mathbf{Q}} = -\frac{\sqrt{N} \tilde{h}}{\tilde{\omega}_{\mathbf{q}}} \delta_{\mathbf{q},\mathbf{Q}}. \quad (\text{A46})$$

Here we have used $\langle B_{\mathbf{q}}^\dagger \rangle_{\tilde{\mathcal{H}}} = 0$. $f^B(\tilde{\omega}_{\mathbf{q}})$ is the bosonic distribution function. Inserting Eqs. (A45) and (A46) into Eqs. (A43) and (A44), one finally arrives at

$$\begin{aligned} n_{\mathbf{q}}^B &= |\tilde{z}_{\mathbf{q}}|^2 f^B(\tilde{\omega}_{\mathbf{q}}) + \frac{1}{N} \sum_{\mathbf{k}} [|\tilde{v}_{\mathbf{k},-\mathbf{q}}^+|^2 \tilde{n}_{\mathbf{k}}^f (1 - \tilde{n}_{\mathbf{k}-\mathbf{q}}^c) \\ &+ |\tilde{v}_{\mathbf{k}\mathbf{q}}^-|^2 \tilde{n}_{\mathbf{k}+\mathbf{q}}^c (1 - \tilde{n}_{\mathbf{k}}^f)]. \end{aligned} \quad (\text{A47})$$

Note that the electronic order parameter $d_{\mathbf{k}}$ and the phononic order parameter Δ are intimately related. Due to Eqs. (A38) and (A41), $d_{\mathbf{k}}$ is proportional to $\tilde{\Delta} = \Delta$, so that both order parameters are mutually dependent. Finally, as a side remark, note that the lattice displacement in the EI state is given by

$$x_{\mathbf{Q}} = \frac{1}{\sqrt{N}} \frac{\tilde{z}_{\mathbf{Q}}}{\sqrt{2\tilde{\omega}_{\mathbf{Q}}}} \langle b_{-\mathbf{Q}}^\dagger + b_{\mathbf{Q}} \rangle_{\tilde{\mathcal{H}}} = -\sqrt{\frac{2}{\tilde{\omega}_{\mathbf{Q}}}} \frac{\tilde{h} \tilde{z}_{\mathbf{Q}}}{\tilde{\omega}_{\mathbf{Q}}}, \quad (\text{A48})$$

as follows from Eqs. (A44) and (A46).

4. Spectral functions

Let us first evaluate the electronic one-particle spectral functions. Here, the c -electron spectral function $A_{\mathbf{k}}^c(\omega)$ was defined before in Eq. (24):

$$A_{\mathbf{k}}^c(\omega) = \frac{1}{2\pi} \int_{-\infty}^{\infty} \langle [c_{\mathbf{k}\sigma}(t), c_{\mathbf{k}\sigma}^\dagger]_+ \rangle e^{i\omega t} dt,$$

where the expectation value is formed with \mathcal{H} . Using the unitary invariance of operator expressions under a trace, one arrives at the former expression Eq. (30). By use of Eqs. (A22)

and (A33) the following result for $A_{\mathbf{k}}^c(\omega)$ is found:

$$A_{\mathbf{k}}^c(\omega) = |\tilde{x}_{\mathbf{k}}|^2 [\xi_{\mathbf{k}-\mathbf{Q}}^2 \delta(\omega - \tilde{E}_{\mathbf{k}-\mathbf{Q}}^1) + \eta_{\mathbf{k}-\mathbf{Q}}^2 \delta(\omega - \tilde{E}_{\mathbf{k}-\mathbf{Q}}^2)] \\ + \frac{1}{N} \sum_{\mathbf{q}} [|\tilde{t}_{\mathbf{k}-\mathbf{q},\mathbf{q}}^+|^2 (\tilde{n}_{-\mathbf{q}}^B + \tilde{n}_{\mathbf{k}-\mathbf{q}}^f) \delta(\omega - \tilde{\varepsilon}_{\mathbf{k}-\mathbf{q}}^f + \tilde{\omega}_{-\mathbf{q}}) \\ + |\tilde{t}_{\mathbf{k}-\mathbf{q},\mathbf{q}}^-|^2 (1 + \tilde{n}_{\mathbf{q}}^B - \tilde{n}_{\mathbf{k}-\mathbf{q}}^f) \delta(\omega - \tilde{\varepsilon}_{\mathbf{k}-\mathbf{q}}^f - \tilde{\omega}_{\mathbf{q}})]. \quad (\text{A49})$$

Similarly, for the f -electron spectral function one finds

$$A_{\mathbf{k}}^f(\omega) = |\tilde{y}_{\mathbf{k}}|^2 [\eta_{\mathbf{k}}^2 \delta(\omega - \tilde{E}_{\mathbf{k}}^1) + \xi_{\mathbf{k}}^2 \delta(\omega - \tilde{E}_{\mathbf{k}}^2)] \\ + \frac{1}{N} \sum_{\mathbf{q}} [|\tilde{u}_{\mathbf{k}\mathbf{q}}^+|^2 (1 + \tilde{n}_{-\mathbf{q}}^B - \tilde{n}_{\mathbf{k}+\mathbf{q}}^c) \delta(\omega - \tilde{\varepsilon}_{\mathbf{k}+\mathbf{q}}^c - \tilde{\omega}_{-\mathbf{q}}) \\ + |\tilde{u}_{\mathbf{k}\mathbf{q}}^-|^2 (\tilde{n}_{-\mathbf{q}}^B + \tilde{n}_{\mathbf{k}+\mathbf{q}}^c) \delta(\omega - \tilde{\varepsilon}_{\mathbf{k}+\mathbf{q}}^c + \tilde{\omega}_{\mathbf{q}})]. \quad (\text{A50})$$

The first line in both spectral functions is the coherent contribution which describes excitations at the electronic quasiparticle energies $\tilde{E}_{\mathbf{k}}^{(1,2)}$. The remaining lines are incoherent contributions. They are induced by the electron-phonon interaction and turn out to be small. Note that the coherent parts in both cases reduce to the mean-field result, when the renormalized quantities are replaced by the unrenormalized quantities.

The phonon spectral function $C_{\mathbf{q}}(\omega)$ is found in the same way. It is defined by

$$C_{\mathbf{q}}(\omega) = \frac{1}{2\pi\omega} \int_{-\infty}^{\infty} \langle [b_{\mathbf{q}}(t), b_{\mathbf{q}}^\dagger] \rangle e^{i\omega t} dt, \quad (\text{A51})$$

where the expectation value is again formed with the full Hamiltonian. Using again the unitary invariance, one finds by help of Eqs. (A22) and (A35)

$$C_{\mathbf{q}}(\omega) = \frac{|\tilde{z}_{\mathbf{q}}|^2}{\tilde{\omega}_{\mathbf{q}}} \delta(\omega - \tilde{\omega}_{\mathbf{q}}) \\ + \frac{1}{N} \sum_{\mathbf{k}} \left[|\tilde{v}_{\mathbf{k},-\mathbf{q}}^+|^2 \frac{\tilde{n}_{\mathbf{k}-\mathbf{q}}^c - \tilde{n}_{\mathbf{k}}^f}{\tilde{\varepsilon}_{\mathbf{k}}^f - \tilde{\varepsilon}_{\mathbf{k}-\mathbf{q}}^c} \delta(\omega - \tilde{\varepsilon}_{\mathbf{k}}^f + \tilde{\varepsilon}_{\mathbf{k}-\mathbf{q}}^c) \right. \\ \left. + |\tilde{v}_{\mathbf{k}\mathbf{q}}^-|^2 \frac{\tilde{n}_{\mathbf{k}}^f - \tilde{n}_{\mathbf{k}+\mathbf{q}}^c}{\tilde{\varepsilon}_{\mathbf{k}+\mathbf{q}}^c - \tilde{\varepsilon}_{\mathbf{k}}^f} \delta(\omega - \tilde{\varepsilon}_{\mathbf{k}+\mathbf{q}}^c + \tilde{\varepsilon}_{\mathbf{k}}^f) \right]. \quad (\text{A52})$$

The first term on the right-hand side describes a coherent phonon with excitation energy at $\omega = \tilde{\omega}_{\mathbf{q}}$. The remaining terms are incoherent contributions due to particle-hole excitations of c and f electrons. As before, they are induced by the electron-phonon interaction. Note that result Eq. (A52) reduces to the mean field result from Sec. III, when the incoherent part is neglected and the coherent excitation energy $\tilde{\omega}_{\mathbf{q}}$ is replaced by the unrenormalized energy ω_0 and $\tilde{z}_{\mathbf{q}}$ by one. The numerical evaluation of $C_{\mathbf{q}}(\omega)$ shows that the weight of the incoherent excitation is small. This allows us to use the energies $\tilde{\varepsilon}_{\mathbf{k}}^c$ and $\tilde{\varepsilon}_{\mathbf{k}}^f$ in expression Eq. (A52) instead of the correct quasiparticle energies $\tilde{E}_{\mathbf{k}}^{(1,2)}$.

The numerical solution of the phonon spectral function in Fig. 7 has shown that $\tilde{\omega}_{\mathbf{q}}$ hardens in the nonadiabatic case ($\omega_0 = 2.5$), whereas it softens in the adiabatic case ($\omega_0 = 0.5$). One may ask, can this opposite tendency of the phonon mode already be understood in perturbation theory? At first, note that ω_0 is not altered by the mean-field theory, as shown in Sec. III. Therefore, the renormalization of the phonon frequency as well as the \mathbf{q} dependence of $\tilde{\omega}_{\mathbf{q}}$ can only be caused by the coupling to the electronic degrees of freedom, i.e., by the influence of \mathcal{H}_1 . The easiest way to derive $\tilde{\omega}_{\mathbf{q}}$ in perturbation theory is to start from the renormalization equation Eq. (A13) for $\omega_{\mathbf{q},\lambda}$, when the renormalization from the original cutoff Λ to $\lambda = 0$ is done in one single step. Therefore, choosing $\lambda = \Lambda$ and also $\Delta\lambda = \Lambda$, one finds from Eq. (A13)

$$\tilde{\omega}_{\mathbf{q}} - \omega_0 = -\frac{2g^2}{N} \sum_{\mathbf{k}} (A_{\mathbf{k},-\mathbf{q}}^+(\Lambda, \Lambda)(n_{\mathbf{k}}^f - n_{\mathbf{k}-\mathbf{q}}^c) \\ + A_{\mathbf{k},\mathbf{q}}^-(\Lambda, \Lambda)(n_{\mathbf{k}}^f - n_{\mathbf{k}+\mathbf{q}}^c)) \\ = -\frac{2g^2}{N} \sum_{\mathbf{k}} \left(\frac{n_{\mathbf{k}}^f - n_{\mathbf{k}-\mathbf{q}}^c}{\varepsilon_{\mathbf{k}-\mathbf{q}}^c - \varepsilon_{\mathbf{k}}^f + \omega_0} + \frac{n_{\mathbf{k}}^f - n_{\mathbf{k}+\mathbf{q}}^c}{\varepsilon_{\mathbf{k}+\mathbf{q}}^c - \varepsilon_{\mathbf{k}}^f - \omega_0} \right), \quad (\text{A53})$$

which is the perturbative result up to $\mathcal{O}(g^2)$. Here we have used that according to Eq. (A9) the coefficients $A_{\mathbf{k}\mathbf{q}}^{\pm}(\Lambda, \Lambda)$ reduce to $A_{\mathbf{k}\mathbf{q}}^{\pm}(\Lambda, \Lambda) = 1/(\varepsilon_{\mathbf{k}-\mathbf{q}}^c - \varepsilon_{\mathbf{k}}^f \pm \omega_0)$.

In the antiadiabatic case ($\omega_0 \gg \varepsilon_{\mathbf{k}-\mathbf{q}}^c, \varepsilon_{\mathbf{k}}^f$), Eq. (A53) reduces to

$$\tilde{\omega}_{\mathbf{q}} = \omega_0 + \frac{2g^2}{N\omega_0} \sum_{\mathbf{k}} (n_{\mathbf{k}-\mathbf{q}}^c + n_{\mathbf{k}+\mathbf{q}}^c). \quad (\text{A54})$$

Since the second term on the right-hand side is positive one indeed finds a hardening of the phonon mode. In the opposite limit ($\omega_0 \ll \varepsilon_{\mathbf{k}-\mathbf{q}}^c, \varepsilon_{\mathbf{k}}^f$) the frequency ω_0 can be neglected in both denominators of Eq. (A53). Then one arrives at

$$\tilde{\omega}_{\mathbf{q}} = \omega_0 - \frac{2g^2}{N} \sum_{\mathbf{k}} \left(\frac{n_{\mathbf{k}}^f - n_{\mathbf{k}-\mathbf{q}}^c}{\varepsilon_{\mathbf{k}-\mathbf{q}}^c - \varepsilon_{\mathbf{k}}^f} + \frac{n_{\mathbf{k}}^f - n_{\mathbf{k}+\mathbf{q}}^c}{\varepsilon_{\mathbf{k}+\mathbf{q}}^c - \varepsilon_{\mathbf{k}}^f} \right). \quad (\text{A55})$$

Note that the second term on the right-hand side is negative. Thus, the result is a softening of the phonon mode in the adiabatic limit, which is like the result in the antiadiabatic limit in agreement with the numerical outcome from the full PRM calculation.

For the numerical evaluation of the various physical quantities from Sec. V within the PRM one has to solve the sets of renormalization equations Eqs. (A11)–(A15) for the parameters of \mathcal{H}_{λ} self-consistently together with the set Eqs. (A26)–(A31) for the expectation values. Starting with some initial values of $n_{\mathbf{k}}^c$, $n_{\mathbf{k}}^f$, $n_{-\mathbf{q}}^B$, and $\langle c_{\mathbf{k}+\mathbf{Q}}^{\dagger} f_{\mathbf{k}} \rangle$, the renormalization equations are integrated in steps $\Delta\lambda$ little by little until, at $\lambda = 0$, the Hamiltonian and all quasiparticle operators are completely renormalized and the new expectation values can be calculated. Then the renormalization process is restarted. Convergence is assumed to be achieved

if all quantities are determined with a relative error less than 10^{-5} . The spectral functions are evaluated with a Gaussian energy broadening of $0.06 t^c = 1$. In the numerics, we have used a one-dimensional lattice with $N = 1000$ sites. $\Delta\lambda$ was customarily chosen as $\Delta\lambda \approx 0.01$ (if we use $\Delta\lambda = 0.1$ in order to reduce the computational effort the discrepancy is proven to be small, however). Concerning the parametrization of the band structure, we choose $\varepsilon^f - \varepsilon^c = -1$ (where ε^c was fixed to $\varepsilon^c = 0$) and $t^f = -0.3$ to ensure an (indirect) semimetallic state for the noninteracting half-filled band case (cf. Fig. 1).

APPENDIX B: ANTIADIABATIC LIMIT

In the antiadiabatic limit the phonon frequency is assumed to be large compared to the electronic energies, $\omega_0 \gg \varepsilon_{\mathbf{k}}^f, \varepsilon_{\mathbf{k}}^c$. One realizes that the renormalization due to the elimination of \mathcal{H}_1 becomes rather small in this limit. This follows from expression Eq. (A8) for $X_{\lambda, \Delta\lambda}$, which has coefficients

$$A_{\mathbf{kq}}^{\pm}(\lambda, \Delta\lambda) = \frac{\Theta_{\mathbf{kq}, \lambda}^{\pm}(1 - \Theta_{\mathbf{kq}, \lambda - \Delta\lambda}^{\pm})}{\varepsilon_{\mathbf{k}+\mathbf{q}, \lambda}^c - \varepsilon_{\mathbf{k}, \lambda}^f \pm \omega_{\mp\mathbf{q}, \lambda}}. \quad (\text{B1})$$

For large $\omega_{\mathbf{q}, \lambda} \sim \mathcal{O}(\omega_0)$, expression Eq. (B1) reduces to

$$A_{\mathbf{kq}}^{\pm}(\lambda, \Delta\lambda) \approx \frac{\Theta_{\mathbf{kq}, \lambda}^{\pm}(1 - \Theta_{\mathbf{kq}, \lambda - \Delta\lambda}^{\pm})}{\pm\omega_0}, \quad (\text{B2})$$

where the Θ functions are now independent of \mathbf{k} :

$$\Theta_{\mathbf{kq}, \lambda}^{\pm} \approx \Theta(\lambda - |\omega_0|) =: \Theta_{\mathbf{q}, \lambda}. \quad (\text{B3})$$

Obviously, for large energy ω_0 , Eq. (B2) only allows small renormalization contributions. Moreover, the product $\Theta_{\mathbf{q}, \lambda}(1 - \Theta_{\mathbf{q}, \lambda - \Delta\lambda})$ in the numerator prevents any \mathbf{k} -dependent renormalization contribution between cutoff λ and $\lambda - \Delta\lambda$.

1. Gap equation

For the conditional equation of the order parameter Δ , obtained by the PRM, one concludes that in the antiadiabatic limit it reduces to the mean-field expression Eq. (23) since renormalization contributions due to \mathcal{H}_1 are suppressed. Thus,

for $\omega_0 \rightarrow \infty$ one obtains as asymptotic result

$$1 = \frac{4g^2}{\omega_0} \frac{1}{N} \sum_{\mathbf{k}} \text{sgn}(\varepsilon_{\mathbf{k}}^f - \varepsilon_{\mathbf{k}+\mathbf{Q}}^c) \frac{f^F(E_{\mathbf{k}}^{(1)}) - f^F(E_{\mathbf{k}}^{(2)})}{W_{\mathbf{k}}}, \quad (\text{B4})$$

where all quantities are unrenormalized.

At the critical electron-phonon coupling $g = g_c$ the order parameter Δ vanishes and the condition Eq. (B4) becomes

$$1 = \frac{4g_c^2}{\omega_0} \frac{1}{N} \sum_{\mathbf{k}} \frac{f^F(\varepsilon_{\mathbf{k}}^f) - f^F(\varepsilon_{\mathbf{k}+\mathbf{Q}}^c)}{\varepsilon_{\mathbf{k}+\mathbf{Q}}^c - \varepsilon_{\mathbf{k}}^f}. \quad (\text{B5})$$

In this extreme antiadiabatic limit, the squared critical coupling g_c^2 scales linearly with ω_0 , provided the electronic parameters in the sum over \mathbf{k} are kept constant. This behavior is in perfect agreement with the outcome from the numerical solution of the PRM equations, as shown in the inset of Fig. 5. Even the numerical result from Eq. (B4) (g_c^2/ω_0) $_{\omega_0 \rightarrow \infty} \simeq 0.16$ is in acceptable agreement with that from Sec. V, which is (g_c^2/ω_0) $_{\omega_0 \rightarrow \infty} \simeq 0.14$.

2. Incoherent excitations

The above feature of $A_{\mathbf{kq}}^{\pm}(\lambda, \Delta\lambda)$ can also be used to explain the behavior of the incoherent contributions to the electronic spectral functions $A_{\mathbf{k}}^{(c,f)}(\omega)$ in Figs. 5 and 6. As long as the electron-phonon coupling g is not too small, the figures show that for the nonadiabatic case ($\omega_0 = 2.5$) in Fig. 6 the incoherent contributions to the spectral functions are less pronounced than for the adiabatic case ($\omega_0 = 0.5$) in Fig. 5. This property results from the prefactors $|\tilde{u}_{\mathbf{k}-\mathbf{q}, \mathbf{q}}^{\pm}|^2$ and $|\tilde{u}_{\mathbf{k}, \mathbf{q}}^{\pm}|^2$ of the incoherent contributions in Eqs. (A51) and (A52). They are found from the solution of the renormalization equations Eqs. (A26) and (A27) for $t_{\mathbf{k}-\mathbf{q}, \mathbf{q}, \lambda}^{\pm}$ and $u_{\mathbf{k}, \mathbf{q}, \lambda}^{\pm}$ and are governed by the coefficients $A_{\mathbf{kq}}^{\pm}(\lambda, \Delta\lambda)$. A similar behavior is also observed for the phonon spectral function $C_{\mathbf{q}}(\omega)$ in Fig. 7, where the incoherent contributions in the antiadiabatic regime are strongly suppressed. Note that also the weight of the incoherent excitations increases when the coupling g is increased.

¹N. Tsuda, K. Nasu, A. Yanase, and K. Siratori, *Electronic Conduction in Oxides* (Springer-Verlag, Berlin, 1991); G. Grüner, *Density Waves in Solids* (Addison Wesley, Reading, 1994).

²R. Peierls, *Quantum Theory of Solids* (Oxford University Press, Oxford, 1955).

³J. E. Hirsch and E. Fradkin, *Phys. Rev. Lett.* **49**, 402 (1982); M. Hohenadler, H. Fehske, and F. F. Assaad, *Phys. Rev. B* **83**, 115105 (2011).

⁴Y. Takada and A. Chatterjee, *Phys. Rev. B* **67**, 081102(R) (2003); H. Fehske, G. Wellein, G. Hager, A. Weiße, and A. R. Bishop, *ibid.* **69**, 165115 (2004); R. T. Clay and R. P. Hardikar, *Phys. Rev. Lett.* **95**, 096401 (2005); M. Tezuka, R. Arita, and H. Aoki, *ibid.* **95**, 226401 (2005); H. Fehske, G. Hager, and E. Jeckelmann, *Europhys. Lett.* **84**, 57001 (2008).

⁵N. F. Mott, *Philos. Mag.* **6**, 287 (1961).

⁶Y. V. Kopaev, *Sov. Phys. Sol. State* **8**, 175 (1966); J. Zittartz, *Phys. Rev.* **165**, 612 (1968).

⁷B. I. Halperin and T. M. Rice, in *Solid State Physics*, edited by F. Seitz, D. Turnbull, and H. Ehrenreich (Academic, New York, 1967), Vol. 21, p. 115; *Rev. Mod. Phys.* **40**, 755 (1968).

⁸F. X. Bronold and H. Fehske, *Phys. Rev. B* **74**, 165107 (2006).

⁹H. Cercellier, C. Monney, F. Clerc, C. Battaglia, L. Despont, M. G. Garnier, H. Beck, P. Aebi, L. Patthey, H. Berger, and L. Forró, *Phys. Rev. Lett.* **99**, 146403 (2007); C. Monney *et al.*, *New J. Phys.* **12**, 125019 (2010).

¹⁰C. D. Batista, *Phys. Rev. Lett.* **89**, 166403 (2002); C. D. Batista, J. E. Gubernatis, J. Bonča, and H. Q. Lin, *ibid.* **92**, 187601 (2004).

¹¹P. Farkašovský, *Phys. Rev. B* **77**, 155130 (2008); C. Schneider and G. Czyczoll, *Eur. Phys. J. B* **64**, 43 (2008); P. M. R. Brydon, *Phys. Rev. B* **77**, 045109 (2008); D. Ihle, M. Pfafferott, E.

- Burovski, F. X. Bronold, and H. Fehske, *ibid.* **78**, 193103 (2008); B. Zenker, D. Ihle, F. X. Bronold, and H. Fehske, *ibid.* **81**, 115122 (2010); K. Seki, R. Eder, and Y. Ohta, *ibid.* **84**, 245106 (2011); D. I. Golosov, *ibid.* **86**, 155134 (2012).
- ¹²V.-N. Phan, K. W. Becker, and H. Fehske, *Phys. Rev. B* **81**, 205117 (2010); V.-N. Phan, H. Fehske, and K. W. Becker, *Europhys. Lett.* **95**, 17006 (2011).
- ¹³B. Zenker, D. Ihle, F. X. Bronold, and H. Fehske, *Phys. Rev. B* **85**, 121102R (2012).
- ¹⁴T. E. Kidd, T. Miller, M. Y. Chou, and T.-C. Chiang, *Phys. Rev. Lett.* **88**, 226402 (2002).
- ¹⁵M. Holt, P. Zschack, H. Hong, M. Y. Chou, and T. C. Chiang, *Phys. Rev. Lett.* **86**, 3799 (2001).
- ¹⁶C. Monney, G. Monney, P. Aebi, and H. Beck, *New J. Phys.* **14**, 075026 (2012); B. Zenker, H. Fehske, H. Beck, C. Monney, and A. R. Bishop, *Phys. Rev. B* **88**, 075138 (2013).
- ¹⁷Recent experiments on $1T$ -TiSe₂ point to a very unusual chiral property of the CDW; see J. Ishioka, Y. H. Liu, K. Shimatake, T. Kurosawa, K. Ichimura, Y. Toda, M. Oda, and S. Tanda, *Phys. Rev. Lett.* **105**, 176401 (2010).
- ¹⁸J. Neuenschwander and P. Wachter, *Phys. Rev. B* **41**, 12693 (1990); B. Bucher, P. Steiner, and P. Wachter, *Phys. Rev. Lett.* **67**, 2717 (1991).
- ¹⁹P. Wachter and B. Bucher, *Physica B* **408**, 51 (2013); E. Burovski, H. Fehske, and A. S. Mishchenko, *Phys. Rev. Lett.* **101**, 116403 (2008).
- ²⁰K. W. Becker, A. Hübsch, and T. Sommer, *Phys. Rev. B* **66**, 235115 (2002); S. Sykora, A. Hübsch, and K. W. Becker, *Europhys. Lett.* **85**, 57003 (2009).
- ²¹A. Zunger and A. J. Freeman, *Phys. Rev. B* **17**, 1839 (1978).
- ²²J. M. Kosterlitz and D. J. Thouless, *J. Phys. C* **6**, 1181 (1973).
- ²³R. J. Bursill, R. H. McKenzie, and C. J. Hamer, *Phys. Rev. Lett.* **83**, 408 (1999).
- ²⁴S. Ejima and H. Fehske, *Europhys. Lett.* **87**, 27001 (2009).
- ²⁵S. Ejima, G. Hager, and H. Fehske, *Phys. Rev. Lett.* **102**, 106404 (2009).
- ²⁶B. Zenker, H. Fehske, H. Beck, C. Monney, and A. R. Bishop, *Phys. Rev. B* **88**, 075138 (2013).
- ²⁷S. Sykora, A. Hübsch, K. W. Becker, G. Wellein, and H. Fehske, *Phys. Rev. B* **71**, 045112 (2005).